3 cys

RECEIVED BY DTIE JUL 29 1970

OK
8/7/60

GEAP-10140
AEC RESEARCH AND
DEVELOPMENT REPORT
JANUARY 1970

MASTER

THE EFFECT OF CYCLIC STRAIN AGING ON THE EMBRITTLEMENT OF A PLAIN CARBON STEEL PLATE

A.J. BROTHERS
D.A. WOODFORD

MATERIALS AND PROCESSES LABORATORY
SCHENECTADY, NEW YORK

U.S. ATOMIC ENERGY COMMISSION
CONTRACT AT(04-3)-189
PROJECT AGREEMENT 37

THIS DOCUMENT CONFIRMED AS
UNCLASSIFIED
DIVISION OF CLASSIFICATION
BY J H Kahn /amh
DATE 8/10/70

P6202

GENERAL ELECTRIC

DISCLAIMER

GEAP-10140
AEC Research and
Development Report
January 1970

THE EFFECT OF CYLIC STRAIN AGING ON THE EMBRITTLEMENT OF A PLAIN CARBON STEEL PLATE

A. J. Brothers
D. A. Woodford

Approved: D H Imhoff
D. H. Imhoff
Manager Development
Engineering

Approved:
S. R. Vandenberg
Project Engineer

Prepared for the
U. S. Atomic Energy Commission
Contract AT (04-3)-189
Project Agreement 37

Printed in U. S. A. Available from the
Clearing House for Federal Scientific and Technical Information
National Bureau of Standards, U. S. Department of Commerce
Springfield, Virginia
Price $3.00 per copy

ATOMIC POWER EQUIPMENT DEPARTMENT • GENERAL ELECTRIC COMPANY
San Jose, California 95125

GENERAL ELECTRIC

DISTRIBUTION OF THIS DOCUMENT IS UNLIMITED

LEGAL NOTICE

TABLE OF CONTENTS

1. **Introduction** 1

2. **Review of Previous Work** 1

3. **General Testing Plan** 2
    - 3.1 Strain Aging in Static Tensile Tests 2
    - 3.2 Embrittlement Following Strain Aging in Cyclic Tension-Compression Tests 2
    - 3.3 Locally Induced Embrittlement in Notch Bend Tests 3

4. **Experimental Procedures** 3
    - 4.1 Materials and Test Specimens 3
    - 4.2 Mechanical Test Procedures 3

5. **Experimental Results** 8
    - 5.1 Strain-Aging in Static Tensile Loading 8
    - 5.2 Strain-Age Embrittlement in Cyclic Loading 8
    - 5.3 Effect of Local Embrittlement in Notch Bend Tests 8

6. **Discussion** 19

7. **Summary and Conclusions** 22

References 22

APPENDIX

A. **Electron Microscopy of Strain-Aged Plain Carbon Steel** 23

References 24

Distribution 30

LIST OF ILLUSTRATIONS

Figure	Title	Page
1	Microstructure of A-212B Carbon Steel Plate Used for Strain-Aging Experiments	5
2	Configuration of Test Specimens	6
3	Schematic Features of Test Specimen and Test Set-Up	7
4	Load-Extension Curves for Carbon Steel (A212B) Specimens at 0.010 In./In./Min Illustrating Serrated or "Saw-Tooth" Curve in Strain-Aging Temperature Range	9
5	Effect of Test Temperature on Ductility and Strength of A-212B Steel Tested in Tension at Various Strain Rates	11
6	Typical Charpy Impact Curves	12
7	Effect of Test Temperature on Charpy Impact and Static Tensile Properties	13
8	Effect of Cyclic Strain at Various Number of Cycles to Shift the Charpy 50% FATT-Reference Condition 50% FATT = 0°F	14
9	Effect of Cycle Strain, Test Temperature and Number of Cycles on Charpy 50% FATT-Reference Condition 50% FATT = 0°F	15
10	Notch Bend Strength at Fracture as a Function of Temperature for Pre-Cyclically Strain-Aged Specimens	17
11	Load-Deflection Curves for Notch Bend Tests	18
12	Correlation of Increase in 50% FATT with Cyclic Strain History Parameter	20
13	Correlation of Charpy 50% FATT with Total Cyclic Strain Range Illustrating Hardness Changes - See Figure 8	21
A-1	Relief Replicas Taken From Close to Fracture of Specimens Deformed in Tension at A) RT B) 300°F and C) 490°F	25
A-2	Effect of Temperature on Dislocation Arrangement After Tensile Deformation. A) RT ~ 20% B) 300°F ~ 10% C) 490°F ~ 15%	26
A-3	Cell Formation Following Fatigue at 350°F A) 37 Cycles at 1.5% B) 200 Cycles at 0.5% C) 200 Cycles at 0.38%	27
A-4	Cell Formation Following Fatigue at RT for 20 Cycles at 0.5%	28
A-5	Elongated Cells Formed After Fatigue at 490°F for 200 Cycles at 0.5%	29

LIST OF TABLES

Table	Title	Page
1	Composition and Mechanical Properties of Experimental Steels	4
2	Tensile Properties of Carbon Steel (A-212B Plate)	10
3	Charpy Impact Properties Following Cyclic and Static Straining Under Various Conditions	16
4	Results of Notch Bend Tests of Locally-Cyclically Strain-Aged Bend Bars	19

ABSTRACT

This report describes the results of static and cyclic strain aging effects on the Charpy impact properties of a carbon steel plate (A-212B). From these results it is concluded that:

a. *Cyclic strain ranges of 0.5 to 3% for up to 200 cycles in the temperature range RT to 550°F increased the Charpy 50% FATT by up to 115°F. The increase in FATT was a direct function of cyclic strain range, number of cycles, and temperature, with maximum embrittlement occurring around 350°F.*

b. *Static deformation was considerably less embrittling than cyclic deformation for equivalent total strain ranges.*

c. *Notch bend tests of 0.050-in. radius, 20% deep notch bend specimens with pre-cyclically strain-aged notch regions revealed no significant influence on nominal notch bend strength.*

1. INTRODUCTION

The effect of *static* or *monotonic* deformation at room or moderately elevated temperature to decrease the notch toughness of carbon steel has been well established.[1-6] It has been observed that the extent of embrittlement as reflected in an increase in the 15 ft-lb energy or 50% fibrous transition temperature (FATT) is a function of the amount of cold deformation prior to aging, or for deformation at moderately elevated temperature is a function both of the amount and temperature of deformation. It has also been shown that embrittlement results from reversed cyclic strain at temperature[7-9]; this embrittlement is nominally attributed to a strain-aging mechanism.

It was the purpose of this investigation to systematically determine the influence of both monotonic and cyclic plastic deformation at temperatures in the strain-aging range on the Charpy impact properties of a carbon steel (A-212B). A secondary purpose was to determine the effect of a locally strain-aged region on the notch bend fracture properties of mildly notched bend bars. Determination of specific temperatures for cyclic strain-aging tests was made following static tensile strain-aging experiments over a range of test temperatures.

2. REVIEW OF PREVIOUS WORK

It has been observed that the ductile-to-brittle transition temperature is increased following *monotonic* deformation either with or without subsequent low-temperature aging. Additionally, it is a function of the extent of deformation and deformation temperature. W. T. Lankford[1] in a summary of the effect of prior cold work on the 15 ft-lb transition temperature of various plain carbon steels observed maximum shifts of about 70°F following cold strains up to 10%. The rate of embrittlement with strain varied with material; in some cases, near-maximum embrittlement occurred at strains of about 1%. Terazawa and Otari[2] observed that the 50% FATT of a 0.14% C, 0.50% Mn steel following both tensile or compressive prestraining at levels to 70% at temperatures in the range of room temperature (RT) to 1300°F increased continuously with strains up to about 50%. For a given strain, the increase in 50% FATT was maximum after deformation in the range 400–600°F. An increase in 50% FATT of 125°F was observed after 5% strain at about 390°F.

This influence of cold or hot deformation on the strength or load-carrying capacity of notched plates and bend bars has been evaluated. Mylonas[3] using a simple bend test of unnotched plate of mild steel, has shown that plastic compression or extension performed at temperatures around 500°F reduced drastically the ductility in subsequent tension at -16°F. Brittle behavior, i.e., fracture at low strains was a function of both deformation temperature and extent Burdekin[4] in a review of this subject reports results of notched 3-inch-square bend bars bent open and reclosed at RT followed by aging 1/2 hour at 482°F. A shift of about 195°F in the temperature of transition from low to high crack opening displacement was observed for several carbon steels; the effect on notch strength was clearly obvious but appeared to be influenced to a lesser degree. Kiefner and Munse[5] in tests of notched plates and bend bars of various low carbon steels found that prestraining at temperatures in the range of 400 to 600°F renders the material at the root of the notch in bend bars susceptible to cracking at loads of about 87% of the yield load. Also, they observed that brittle fracture can initiate at low applied stresses in the vicinity of welds in mild steel plate; this latter effect implies that regions of the parent plate are severely embrittled by the thermal and strain cycles that accompany welding.

Although there are fewer tests of the influence of cyclic strain on the impact and notch strength properties of carbon steels, effects similar to those described above have been observed following reversed cyclic plastic strain at moderately elevated temperatures. Forrest[6] found that a 0.17% C steel cycled at 350°F for 10^7 cycles shifted the Charpy energy curve about 110°F to higher temperature. This shift was considerably greater than that observed for an equivalent and higher static strain at the same temperature. Susukida and Ando[7] for two carbon steels with about 0.18% C found an apparent relation between the 15 ft-lb transition temperature and total plastic strain after cyclic loading at room temperature with no apparent influence of number of cycles. As noted by these authors, the rise in transition temperature was perhaps all or in part associated with an increase in hardness due to hardening during cycling.

A more extensive investigation of the effect of reversed axial strain at RT and 600°F on the Charpy 50% FATT has been performed by Salkin[8] for several high manganese, low-alloy carbon steels. Increases in transition temperature of up to about 144°F were observed following cycling at 300°C (572°F). Similar cycles at RT produced much less embrittlement.

To correlate the influence of strain range and number of cycles, Salkin devised a single parameter derived from consideration of total accumulated strain, i.e.,

$$\frac{n\Delta\epsilon_t^2}{\epsilon_f^2}$$

where

$\Delta\epsilon_t$ = total strain range per cycle, %;
ϵ_f = true fracture strain, %, derived from tensile reduction in area; and
n = number of cycles.

This parameter was then empirically correlated with observed changes in transition temperature, i.e., 50% FATT. It was observed that the change in transition temperature for several low-alloy steels was greater following deformation in the strain-aging range, i.e., 300°C. This parameter and approach if applicable has merit in that it permits an estimate of the extent of embrittlement for strain ranges and number of cycles other than those tested.

Powers[9] in fully reversed strain cycling tests of A302 steel observed an influence of temperature on the stress amplitude to obtain a given strain range, and determined the increase in Charpy impact 50% FATT after various levels of cyclic strain at 600°F. A maximum shift of 90°F was obtained following 300 cycles at a strain range of 1.3%. This increase was approximately the same magnitude as observed by Salkin for this same steel.

Coffin,[10] in tests to determine the influence of cyclic strain on fracture properties of low-carbon steels, observed that the ductility transition temperature, i.e., the temperature corresponding to a sharp drop in tensile reduction in area increased about 200°F following several cycles at ± 1% strain at 250°C (482°F).

3. GENERAL TESTING PLAN

The general testing plan followed is described below.

3.1 STRAIN AGING IN STATIC TENSILE TESTS

To determine the general temperature range of maximum static strain-aging effects, and the influence of strain rate on strain aging response, tensile tests were conducted over the range RT to 600°F at various rates. From these tests, the temperature of maximum strain aging as reflected in an increase in strength and/or a decrease in ductility was determined. These tests were conducted on plates in the nominally stress-relieved condition, i.e., 1050°F for 1 1/2 hours, and for material given a thermal treatment at 1250°F for 2-1/2 hours and water quenched. This latter condition was an attempt to simulate possible fast cooling rates associated with welding or other processes resulting in these thermal effects. To determine the influence of *static* strain-aging on Charpy impact properties, and thus provide a basis for comparison with *cyclically* strain-aged specimens, a few plate specimens were statically strained to various amounts at 350°F and Charpy properties obtained.

3.2 EMBRITTLEMENT FOLLOWING STRAIN AGING IN CYCLIC TENSION-COMPRESSION TESTS

After the above tests, 1-inch-thick plates were cycled over total tension-compression strain ranges of 0.2 to 3.0% for up to 1,000 cycles at a single slow rate of loading at 350°F. Also, a few tests were made at temperatures in the range of RT to 550°F to determine the influence of test temperature including that associated with reactor operation. Charpy impact properties were determined from these plates to measure the shift in transition temperature relative to the virgin plate material.

3.3 LOCALLY INDUCED EMBRITTLEMENT IN NOTCH BEND TESTS

Since it is likely that strain-aging embrittlement, if it were to occur, would be present as a locally embrittled region, it was believed of value to determine whether low stress fracture of a locally embrittled region could trigger fracture in nominally unaffected base metal. For this purpose, mildly notched bend bars were cyclically deformed at 350°F at conditions designed to obtain a shift of 50% FATT of about 100°F. Final loading was in compression to avoid inducing compressive residual stresses. These specimens were then tested at temperatures from -320°F to RT to determine possible influence on notch bend strength properties. For comparison with the above results, a single specimen was tested in the non-cyclically strain-aged conditions.

4. EXPERIMENTAL PROCEDURES

4.1 MATERIALS AND TEST SPECIMENS

The composition and mechanical properties of the experimental material are given in Table 1. These properties as well as the mixed ferrite plus pearlite microstructure shown in Figure 1 are typical for steels of this type and composition.

To establish a reference condition to which the results of various strain-aging cycles could be compared, all experimental material with the few exceptions noted below were stress-relieved at 1050°F for 1-1/2 hours and air cooled. To obtain a uniform and constant metallurgical condition, all cyclic specimens were heated to 350°F for 24 hours prior to test. This treatment which resulted in a 50% FATT of 0°F is considered the reference condition for all subsequent tests.

The configurations of the test specimens used are shown in Figures 2 and 3. These include conventional strip tensile specimens, standard Charpy impact specimens, a notch-bend specimen and a dumbbell-shaped specimen of welded lamellar fabrication. From each of these specimens, a set of Charpy specimens was machined using the orientation shown, i.e., the specimens were transverse with the fracture surface parallel to the direction of rolling, and the length of the specimen perpendicular to the rolling direction.

The notch bend specimen of Figure 3 was employed to determine the effect of local cyclic strain aging on notch bend properties after cycling at 350°F to ± 0.5% strain to pre-embrittle the notch. The arrangements used for cycling and testing this specimen are shown in Figure 3. In all cases, the final loading was in compression to avoid inducing favorable compressive residual stresses at the notch.

4.2 MECHANICAL TEST PROCEDURES

Standard mechanical test procedures were employed in all tests. Rates of loading for the static tensile tests were 0.001 in./in./min, 0.010 in./in./min, and 0.010 in./in./min plus a 30 minute hold time at 1%, 3%, and ultimate tensile strain levels. Since these rates did not exhibit significantly different effects in tensile tests, cyclic strain-aging tests were performed at a rate of 0.002--0.005 in./in./min. Strain ranges for these tests were monitored and controlled over a range of 0.2% to 3% using strain gages attached to both sides of the dumbbell specimen. Cycling was performed to obtain a fixed total strain range, irrespective of amplitude. In some cases, the total range was developed by cyclic excursions of equal amplitude in both tension and compression; in other specimens, cycling was to an amount necessary to restore the specimen to its initial length. There was no apparent influence of this variation in cycling path on subsequent embrittlement.

Heating for the strip tensile tests and cyclic strain-aging tests was performed in heated insulated cabinets. Heating of notch bend bars and statically loaded plate specimens used resistance-heated electrical tapes. In all cases specimen temperature was monitored with a thermocouple embedded 1/4 inch below the surface of the specimen.

Cycling of notch bend bars to induce a locally strain-aged region at the notch was performed in three-point bending over a 7 to 8-inch span in reversed bending for about 200 cycles. The notch-root strain range of cycling was about ± 0.5% as monitored with a 1/32-inch-long gage length strain gage placed in the notch at the mid-thickness of the specimen. This level of strain in subsequent tests was observed to shift the 50% FATT by about 100°F. Thus, the material at the root of the notch can be considered to have a 50% FATT of about 100°F while the FATT of the bulk material is about -10°F. Cycling was completed after a compressive cycle to avoid inducing residual compressive stresses at the notch.

To determine the depth and hardness of the strain-aged notch root region, microscopic examination of bend bars was performed. This examination revealed no clearly discernible plastic strain zone. Microhardness traverses in the vicinity of the notch indicated a locally-hardened zone about 0.100-inch deep.

Fracture tests of cyclically strain-aged notch bend bars, and a few virgin specimens for comparison were made in three-point bend-tension over a span of about 7.5 inches. Cooling was performed with either an alcohol-dry ice mixture (-105°F) or liquid nitrogen (-320°F). For intermediate temperatures, the bar was cooled to -320°F and allowed to heat to the test temperature.

TABLE 1
COMPOSITION AND MECHANICAL PROPERTIES OF EXPERIMENTAL STEELS

Composition	**C**	**Mn**	**P**	**Si**	**S**	**Cu**	**N_2**
(weight percent)	0.24	0.74	0.015	0.24	0.031	0.23	0.007

Grain Size: ASTM No. 6.5
Microstructure - Fine pearlite-ferrite mixture (Figure 1)

Mechanical Properties (Transverse):

Test Temp. (°F)	**Ultimate Strength (psi)**	**0.02% Yield Strength (psi)**	**0.2% Yield Strength (psi)**	**Red. in Area (%)**	**Elong. in 1 in. (%)**
Room	75,883	48,875	44,666	46.1	41.5
125	72,500	44,800	44,700	–	–
200	72,250	–	–	–	–
300	80,250	40,500	41,500	–	–
400	83,400	38,700	39,700	28.5	20.0
500	85,000	30,300	36,700	31.2	31.0

Charpy Impact Properties (Transverse):

As-Received - 1050°F - 1 1/2 hours

Test Temp. (°F)	**Impact Energy (ft-lb)**	**% Fibrous Fracture**
75	27.0	100
25	21.5	94
0	18.5	80
-10	13.0	55
-25	9.0	33
-50	4.0	11

As Received - 1050°F - 1 1/2 hrs. + 350°F - 24 hrs.

Test Temp. (°F)	**Impact Energy (ft-lb)**	**% Fibrous Fracture**
75	25.5	100
0	12.5	52
-25	12.0	38
-50	3.5	12

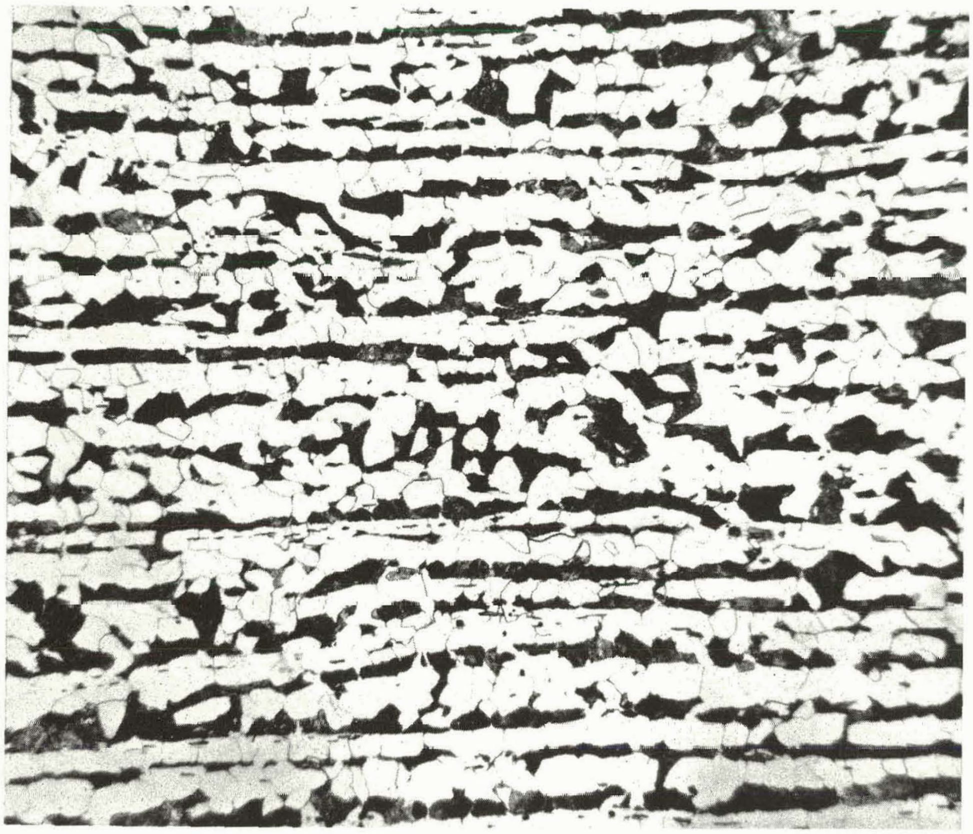

250X

Figure 1. Microstructure of A-212B Carbon Steel Plate Used for Strain-Aging Experiments.

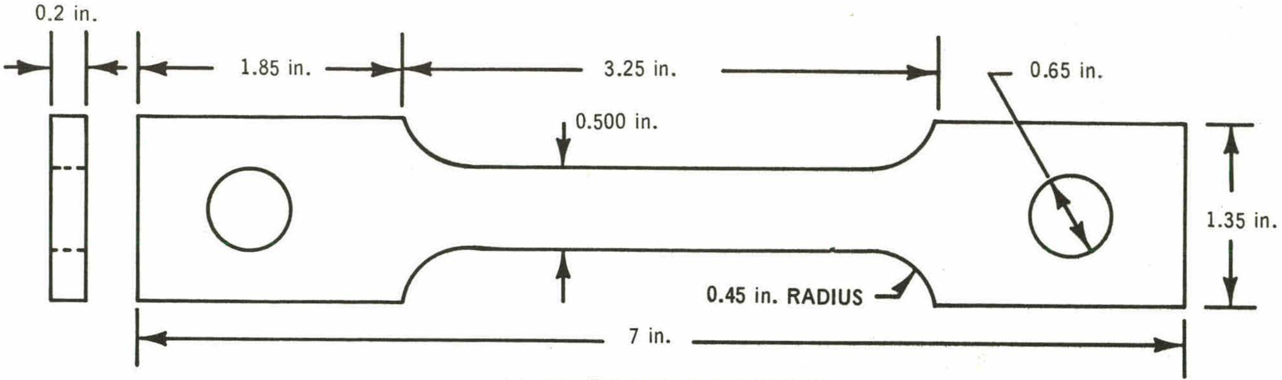

(a) STRIP TENSILE SPECIMENS

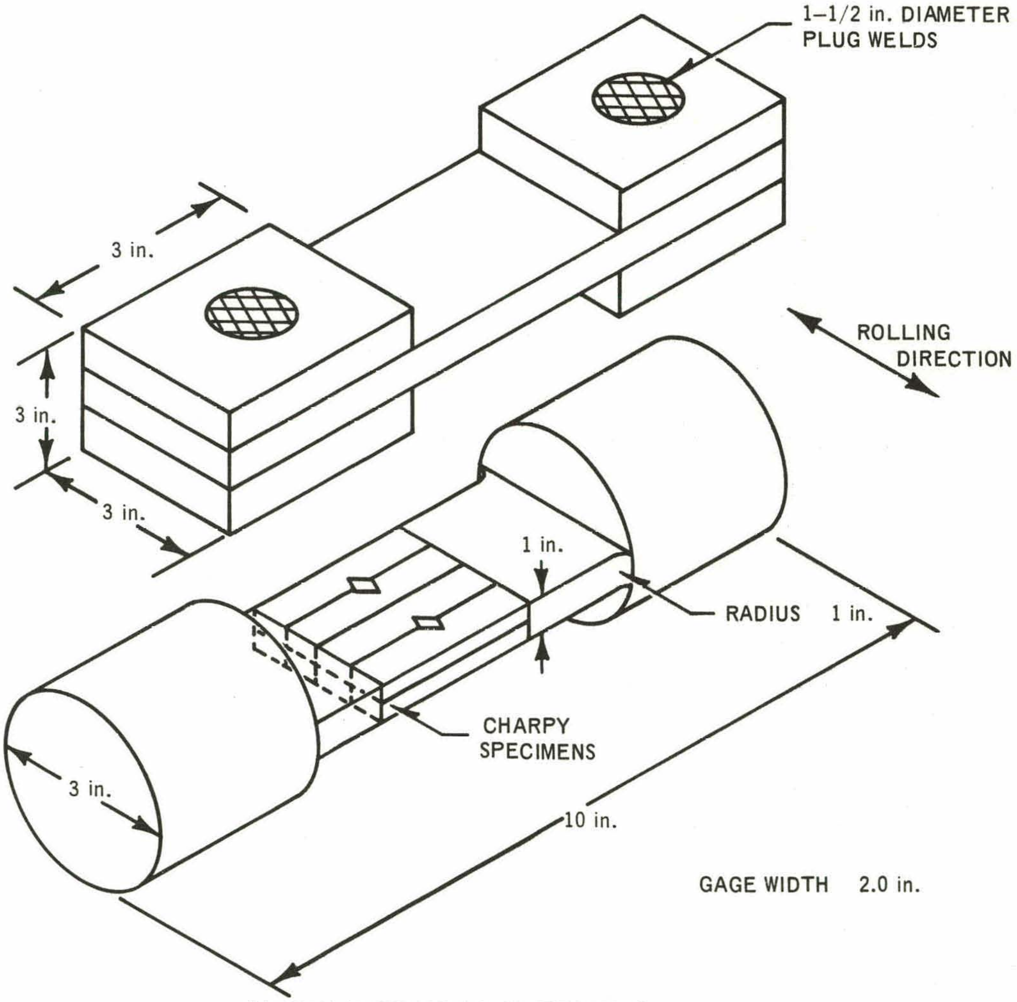

(b) CYCLIC STRAIN AGING SPECIMENS

Figure 2. Configuration of Test Specimens

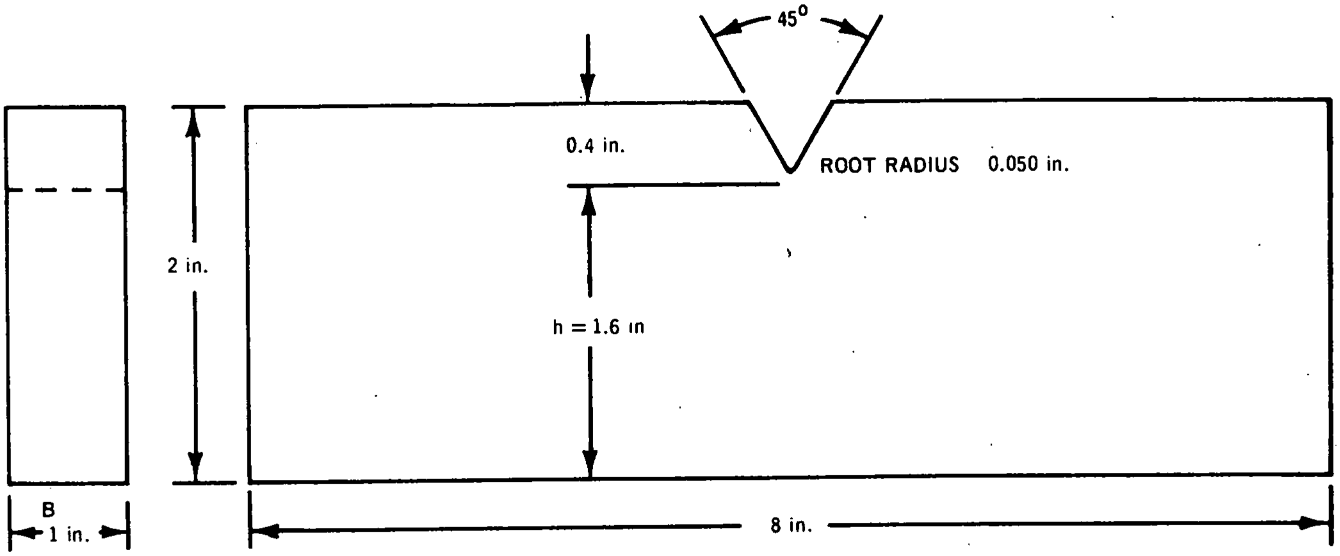

(a) NOTCH BEND TEST SPECIMEN

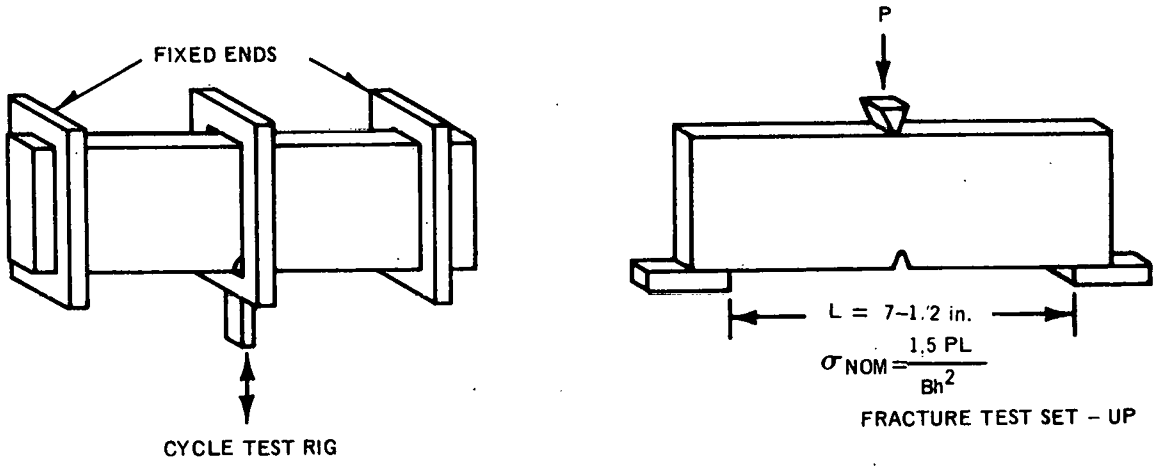

(b) TEST SET–UP

Figure 3. Schematic Features of Test Specimen and Test Set-Up

5. EXPERIMENTAL RESULTS

5.1 STRAIN-AGING IN STATIC TENSILE LOADING

The results of tensile tests throughout the strain-aging temperature range are listed in Table 2 and illustrated in Figures 4 and 5. Figure 4 shows portions of the load-extension curves for the as-received stress-relieved plate, and illustrates the typical serrated or saw-tooth load-extension curve observed for carbon steel in the temperature range of 300 to 400°F. This phenomenon, associated with discontinuous yielding, is evident at 300°F for strains in the yield point region. At 400°F, serrations do not occur at strains near the yield point, but are evident at higher strains.

The ductility and strength properties are shown in Figure 5. These results indicate that the temperature of minimum ductility coincides with that temperature at which serrations are evident in the load-extension curves. The few tests at lower strain rates, including the influence of a hold-time at various strain levels, indicate a minor effect of this variable, but no appreciable effect on the temperature of maximum embrittlement. Figure 5 also illustrates similar effects for material given a thermal treatment at 1250°F for 2-1/2 hours and then water quenched. This treatment generally decreased the absolute level of strength and increased the ductility; however, the temperature of maximum strain-aging was unaffected.

5.2 STRAIN-AGE EMBRITTLEMENT IN CYCLIC LOADING

The results of Charpy impact tests following cyclic strain-aging at various temperatures, cycles and strain ranges are listed in Table 3 and shown in Figures 6 through 9. These results include the temperature at which 15 ft-lb is absorbed, the temperature of 50% fibrous fracture, i.e., 50% FATT, and energy absorbed at 100% fibrous fracture.

Typical raw results of Charpy impact tests following cyclic strain aging at a given condition are shown in Figure 6. These results indicate the effect of strain-aging to both increase the brittle-to-ductile transition temperature, and to decrease the maximum absorbed energy.

As shown in Figure 7, there is, for a given strain range and cyclic history, an apparent influence of test temperature on shift in 50% FATT which is qualitatively similar to that observed in results of tensile tests, Figure 4. The extent of embrittlement increases with increasing test temperature and appears to maximize at 300 to 400°F; there is the suggestion of lesser embrittlement at 550°F. The shift in 15 ft-lb transition temperature illustrates similar effects. However, since the maximum energy level is also affected by cyclic strain-aging, a constant energy criterion may not be as unequivocal as that based on fracture appearance.

The influence of cyclic strain range for various numbers of cycles is shown in Figure 8. These results indicate a significant effect of strain range on embrittlement. Also, as shown in Figure 9, there is for a given strain range, an apparent effect of the number of cycles. Over the strain ranges tested, there is evidence that the Charpy transition temperature for a fixed number of cycles increases continually over the strain range examined. However, the influence of the number of cycles in the range 50 to 100 is relatively weak. The maximum shift in 50% FATT noted was 115°F following 151 cycles at ± 1.0%.

Figure 8 also shows the shift in transition temperature associated with static deformation at 350°F. These latter results, though somewhat questionable for the reasons discussed below, indicate a significantly lesser effect of static than cyclic deformation on embrittlement resulting from strain aging.

5.3 EFFECT OF LOCAL EMBRITTLEMENT IN NOTCH BEND TESTS

The notch bend fracture properties of this steel over the temperature range of -320°F to RT are shown in Figure 10, and listed in Table 4; typical load-deflection curves are shown in Figure 11. These results indicate within scatter that the nominal net section bend strength calculated from the maximum bending load is essentially high and constant over the range RT to -220°F with low strength occurring at -320°F. Comparison of the two tests at -150°F, one of which contained incipient cracks developed during the cyclic straining revealed no appreciable effect of this variable for the conditions tested. Examination of the load-deflection curves, Figure 11, revealed no evidence of incipient or partial fracture associated with a shallow brittle region. In a single test at room temperature, an attempt to detect acoustical emission, i.e., a "ping", using a contact microphone failed to reveal incipient cracking. Whether incipient cracking occurred at low temperatures with insufficient load-drop to provide an indication on the load-deflection curve is uncertain.

For comparison purposes and to evaluate the relative effect of local embrittlement on fracture properties, both a fatigue cracked bend bar (notch plus 0.080-inch-deep fatigue crack, and a virgin bar of mild radius, 0.040 in. was tested at -105°F. These test results (Figure 10) indicate no significant differences in notch strength, and suggest that the cyclically strain-aged region developed in these tests had no influence on notch bend strength.

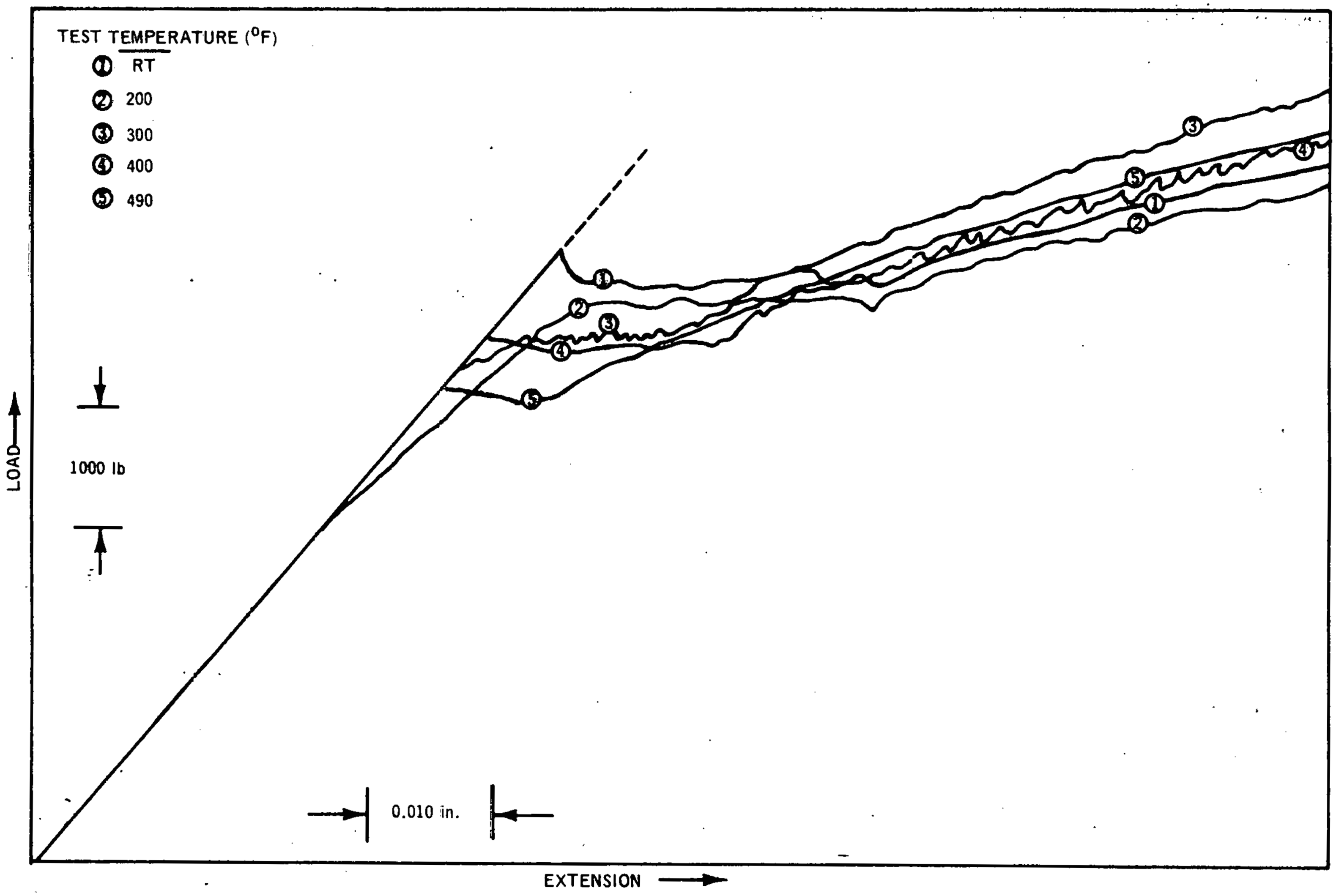

Figure 4. *Load-Extension Curves for Carbon Steel (A212B) Specimens at 0.010 In./In./Min Illustrating Serrated or "Saw-Tooth" Curve in Strain-Aging Temperature Range*

TABLE 2
TENSILE PROPERTIES OF CARBON STEEL (A-212B PLATE)

Spec. No.	Test Temp., (°F)	Upper Yield Strength (ksi)	Lower Yield Strength (ksi)	Ultimate Strength (ksi)	Elong. in 2 in. (%)
Condition - As-Received + Stress Relieved 1050°F - 0.010 in./in./min					
6	Room	49.8	46.7	76.1	32.0
14	200	45.6	44.6	74.5	17.0
1	300	44.6	43.1	85.6	14.5
4	400	40.3	42.3	92.1	18.0
15	490	38.8	37.8	89.2	24.0
Condition - Same as Above - 0.001 in./in./min					
5	300	47.7	44.2	87.7	12.5
2	400	43.2	42.3	94.4	24.0
Condition - Same as Above - 0.010 in./in./min + 30-min hold @ 1%, 3% and strain at maximum load					
7	300	43.5	41.5	85.0	12.5
16	400	43.3	41.1	91.1	15.0
Condition - 1250°F - 2.5 Hours - Water Quenched - 0.010 in./in./min					
17	Room	49.0	46.3	71.6	30.0
13	200	44.9	43.8	71.6	21.5
10	300	43.9	41.4	73.2	19.0
3	400	39.7	36.6	78.0	20.5
11	500	30.6	30.5	74.6	24.0

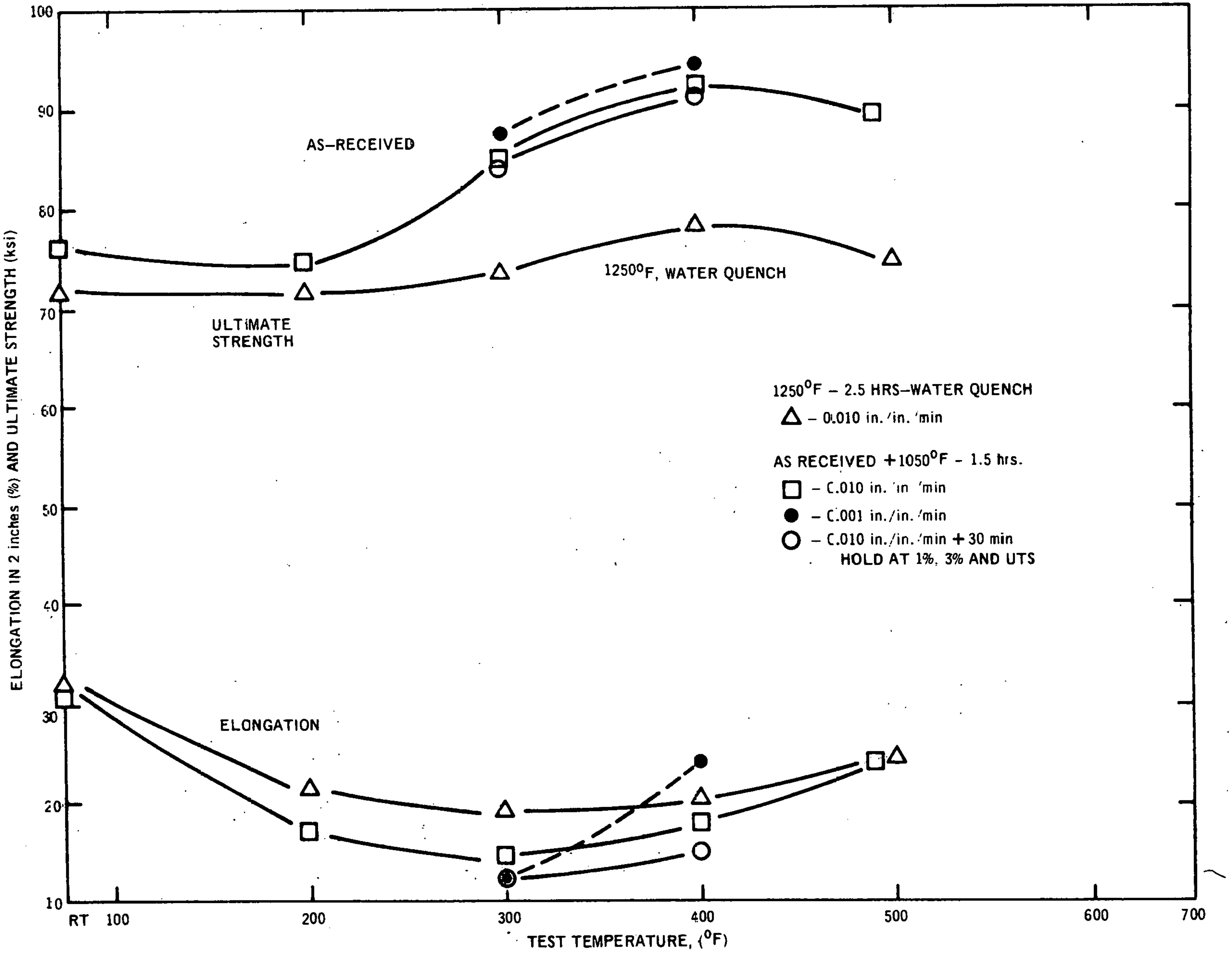

Figure 5. Effect of Test Temperature on Ductility and Strength of A-212B Steel Tested in Tension at Various Strain Rates

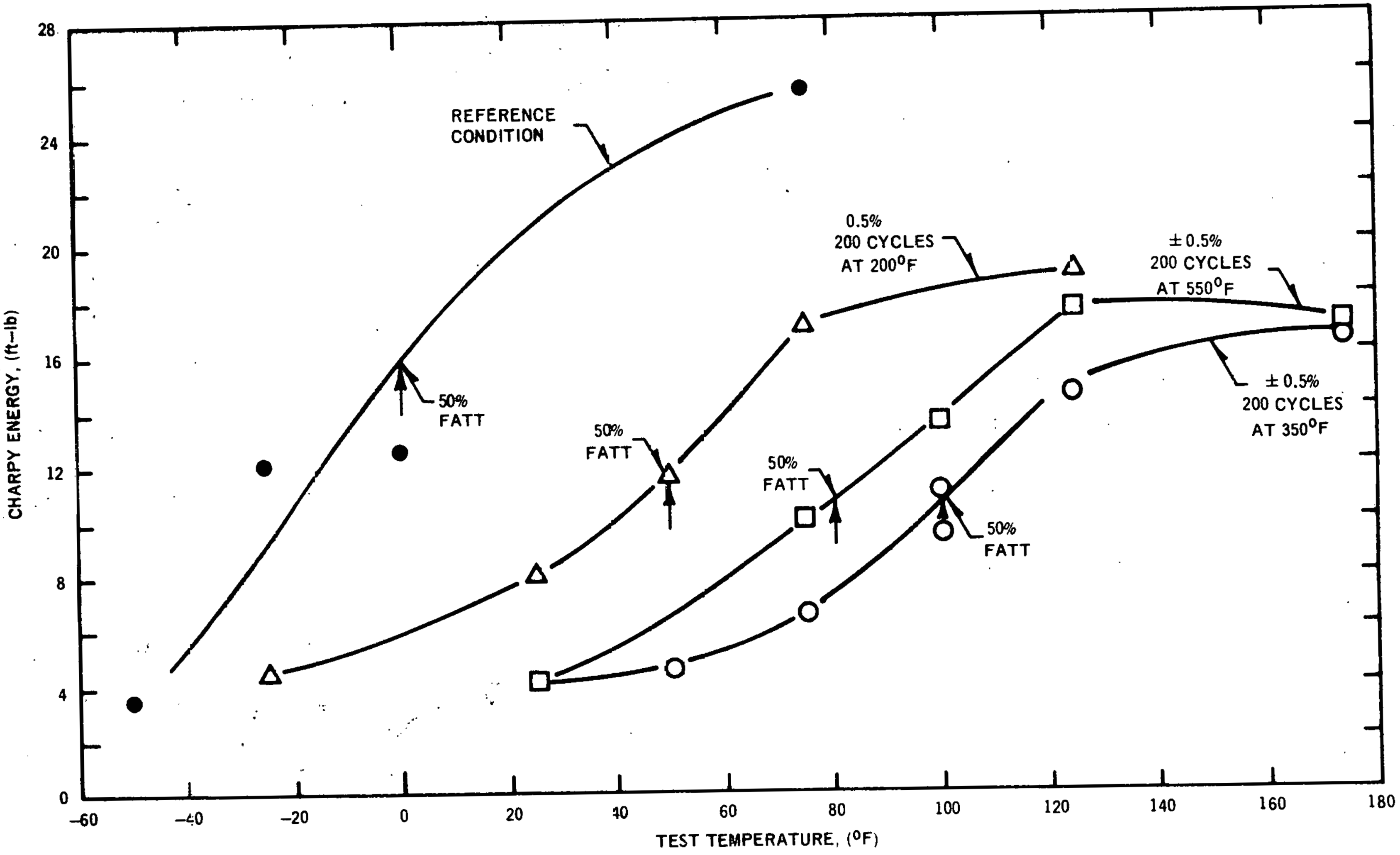

Figure 5. Typical Charpy Impact Curves

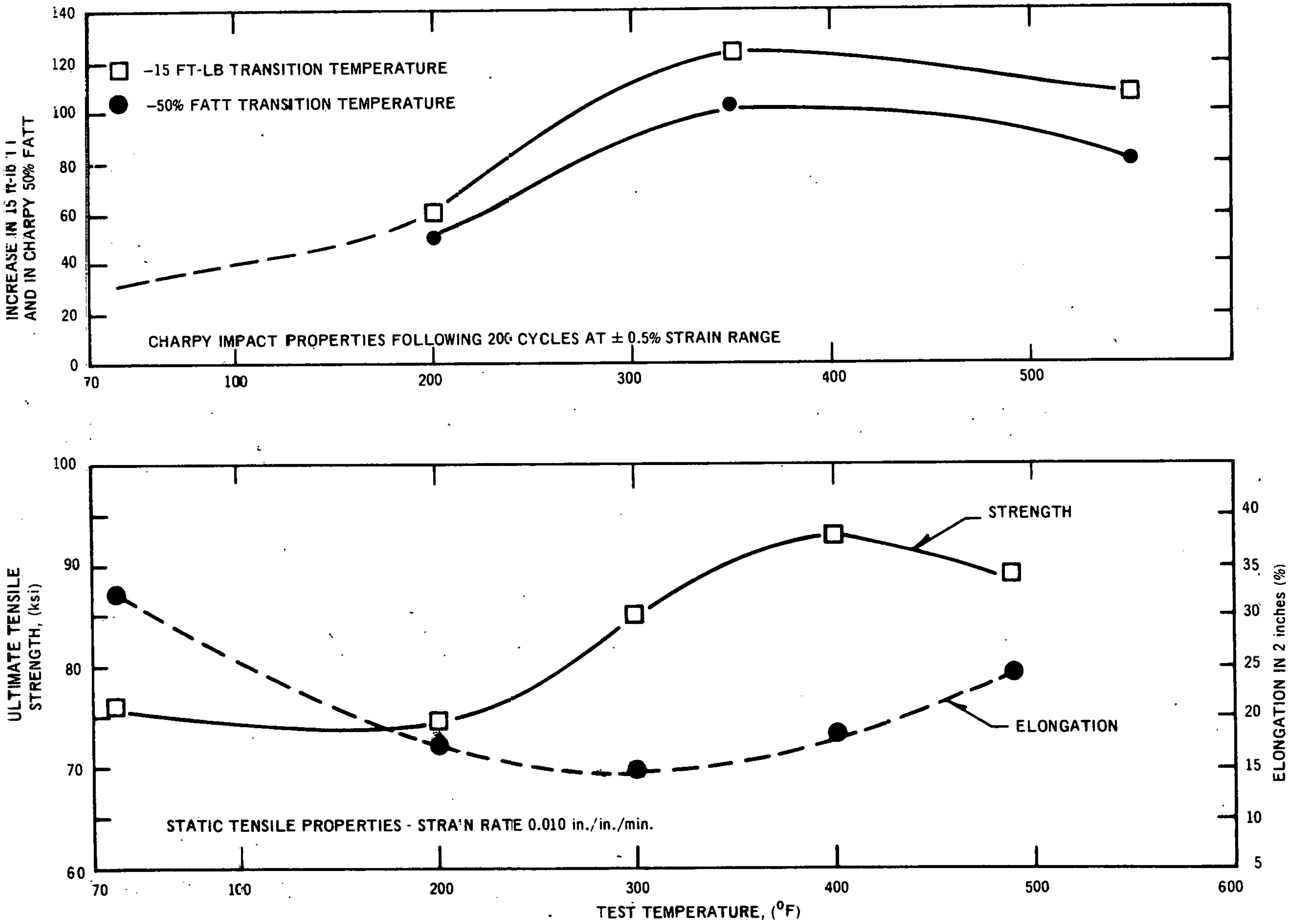

Figure 7. *Effect of Test Temperature on Charpy Impact and Static Tensile Properties*

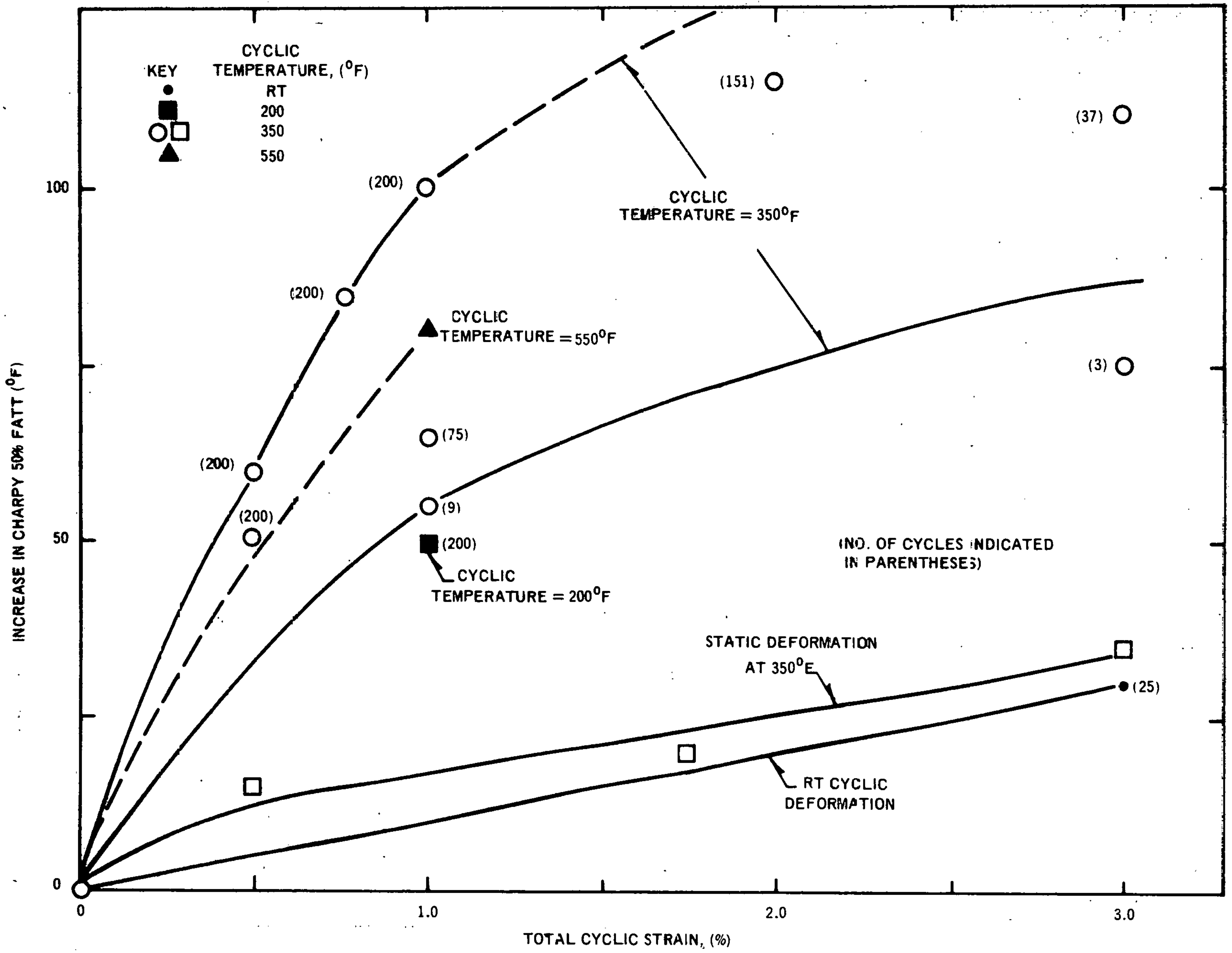

Figure 8. Effect of Cyclic Strain at Various Number of Cycles to Shift the Charpy 50% FATT-Reference Condition 50% FATT= 0°F

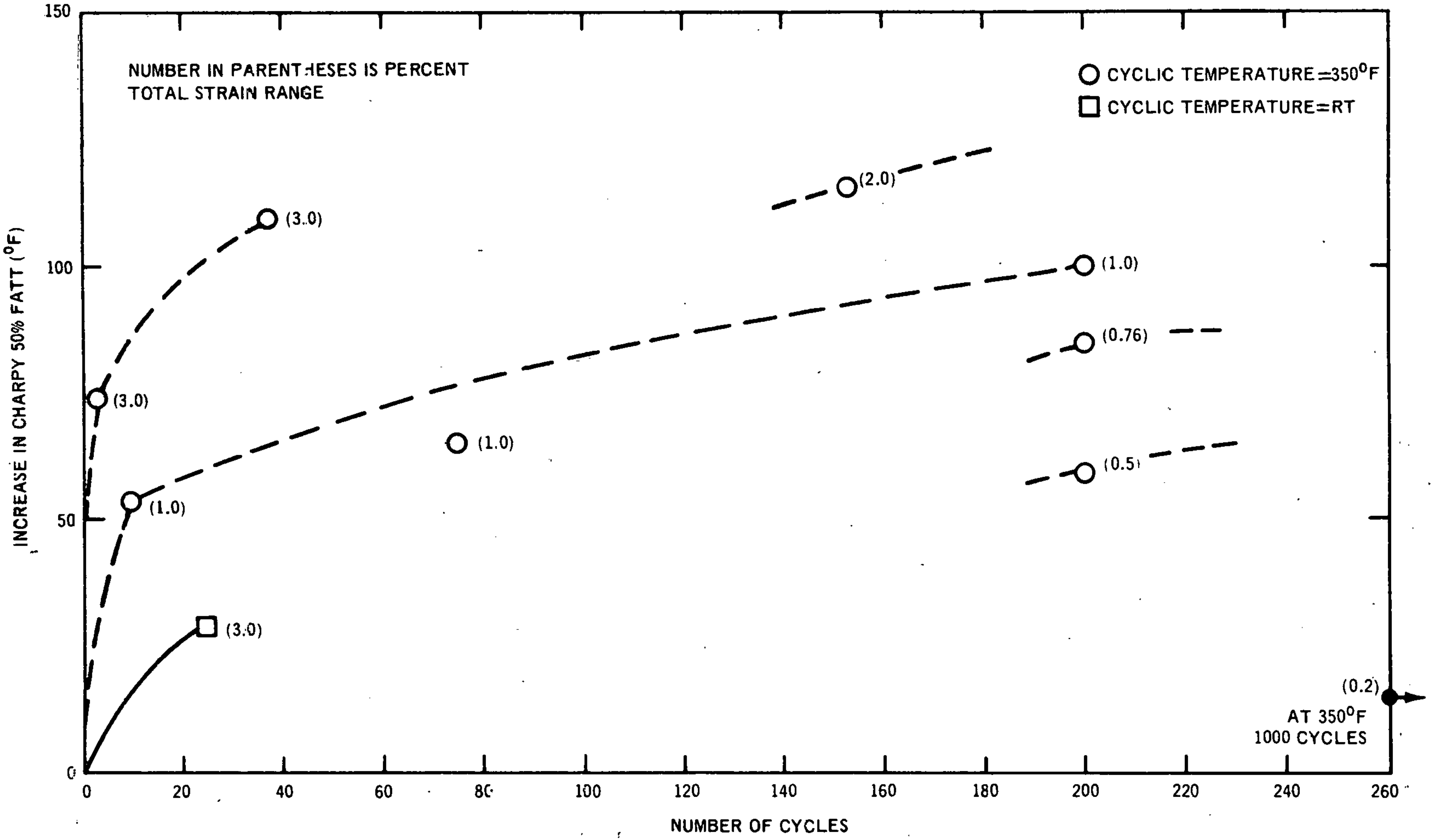

Figure 9. *Effect of Cycle Strain, Test Temperature and Number of Cycles on Charpy 50% FATT-Reference Condition 50% FATT = 0°F*

TABLE 3
CHARPY IMPACT PROPERTIES FOLLOWING CYCLIC AND STATIC STRAINING UNDER VARIOUS CONDITIONS

Condition	Charpy 50% FATT (°F)	15 ft-lb Trans. Temp. (°F)	Max. Energy ft-lb
1. As-received plus	0	+5	25.5
1050°F - 1-1/2 hours	-5	+5	24.5
plus 350°F - 24 hours	0	+5	24.5
	Cycled at RT		
2. ±0.5% - 20 cycles plus ±1.0% - 20 cycles plus ±1.5% - 25 cycles	30	+42	19.0
	Cycled at 200°F		
3. ±0.5% - 200 cycles	50	65	19.0
	Cycled at 350°		
4. ±0.10% - 1000 cycles	-15	-5	23.0
5. ±0.25% - 200 cycles	60	95	18.0
±0.25% - 200 cycles	50	65	22.0
6. ±0.38% - 200 cycles	85	105	17.0
7. ±0.50% - 9 cycles	55	65	20.5
8. ±0.50% - 75 cycles	65	45	36.5
9. ±0.5% - 200 cycles	100	130	16.5
10. ±1.0% - 151 cycles	115	150	15.5
11. ±1.5% - 3 cycles	76	96	19.5
12. ±1.5% - 37 cycles	110	125	16.0
	Cycled at 550°F		
13. ±0.5% - 200 cycles	80	112	17.5
	Statically Deformed @ 350°F		
14. 0.5%	15	10	38.0
15. 1.75%	20	15	41.0
16. 3.00%	35	25	39.5

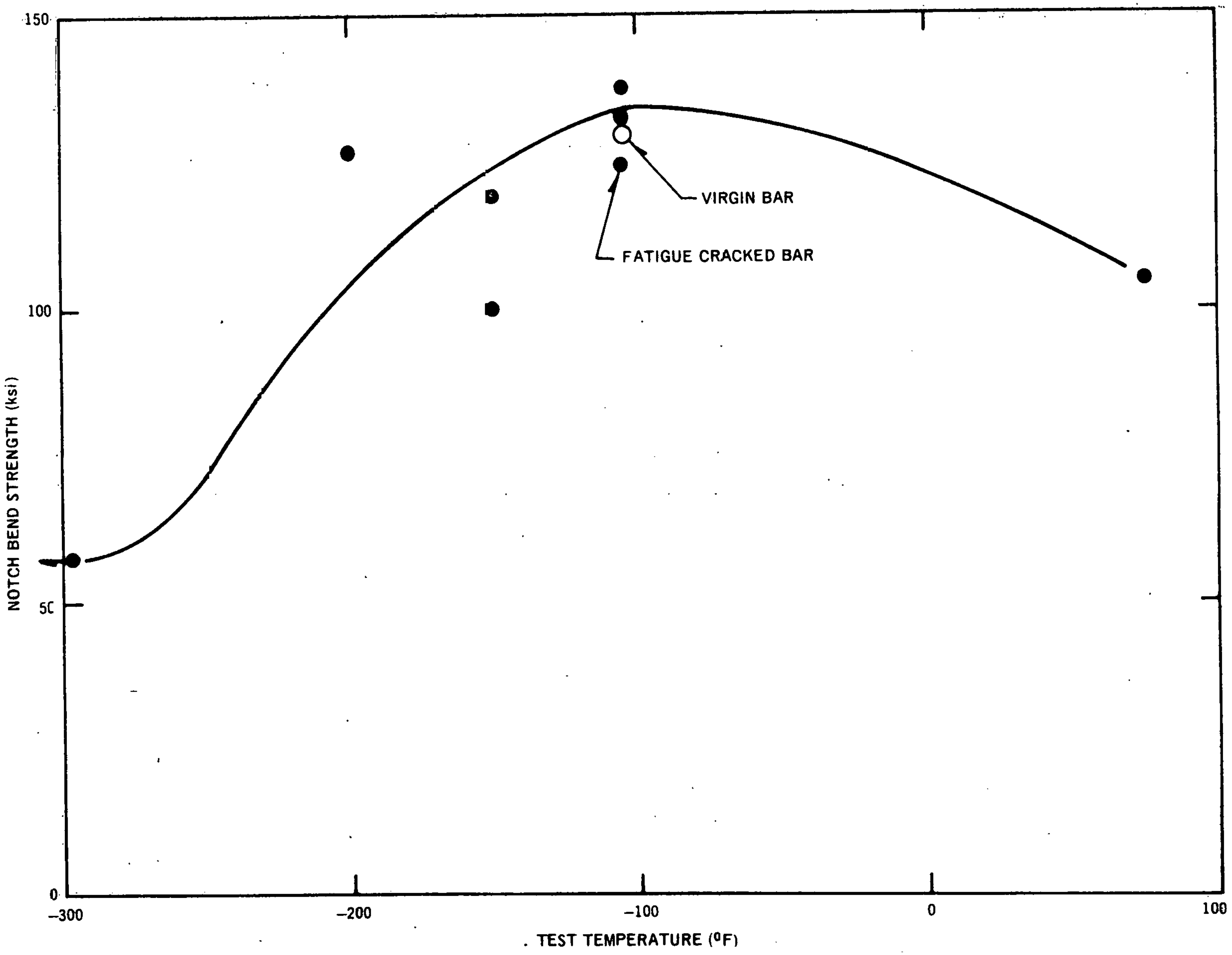

Figure 10. *Notch Bend Strength at Fracture as a Function of Temperature for Pre-Cyclically Strain-Aged Specimens*

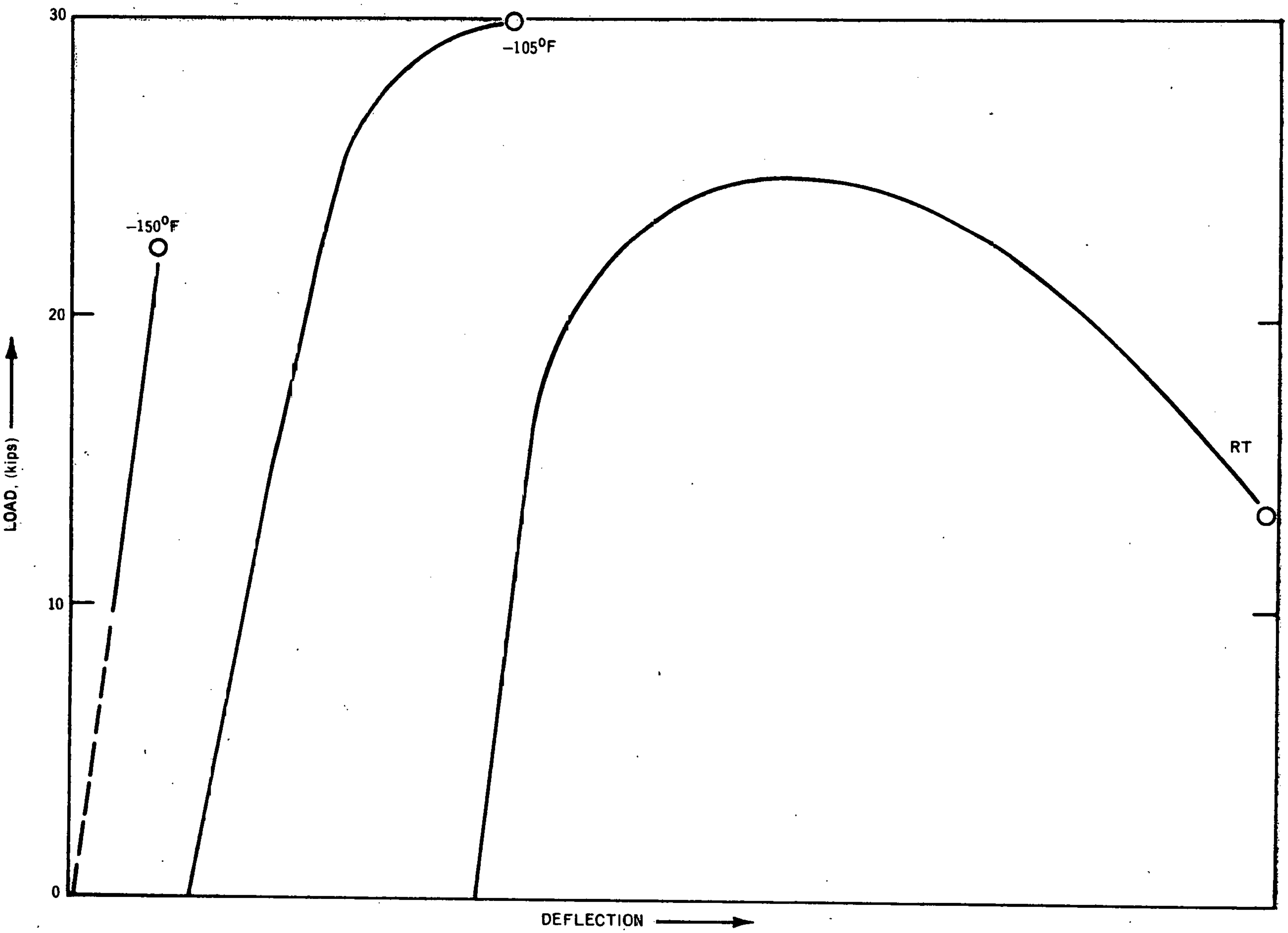

Figure 11. Load-Deflection Curves for Notch Bend Tests

TABLE 4
RESULTS OF NOTCH BEND TESTS OF LOCALLY-CYCLICALLY STRAIN-AGED BEND BARS

Test Temp. (°F)	Incipient Cracks at Notch	Notch Fracture Strength on Net Section (psi)	Total Depth of Fibrous Tear At Notch (in.)
Room	No	105,000	1.6 (100% fibrous)
-105	Yes (0.26 in.)	138,000	0.32
-105	Yes (0.07 in.)	132,500	0
-150	No	100,000	0
-150	Yes (0.01-0.015 in.)	119,700	0
-200	NO	127,600	0
-320	Yes (0.07-0.08 in.)	57,800	0
-105	No, as machined notch - not pre-strain aged	131,000	0.19

6. DISCUSSION

The results of these studies indicate conclusively an embrittling effect of strain aging, the magnitude of which is apparently influenced by test temperature, strain range, and number of cycles. To compare these results with the approach devised by Salkin[8] calculations were made of the parameter $(n\Delta\epsilon_t^2)/(\epsilon_f^2)$.

Since these quantities reflect the influence of strain range ($\Delta\epsilon_t$), number of cycles (n) and, indirectly, test temperature through its effect on tensile reduction in area (ϵ_f), it has possible usefulness for estimating transition temperatures for those conditions of strain and cyclic history not specifically tested. A correlation, and comparison with the original results by Salkin[8] for low-alloy steels tested at 300°C (572°F) is shown in Figure 12. This comparison indicates generally that the rate of embrittlement associated with a given strain range-cycle history is considerably greater in Salkin's tests, but that the general parametric concept appears suitable for correlating these variables, at least within the ranges evaluated in these tests.

To determine whether the apparent increase in transition temperature for these tests possibly resulted from simple hardening as a result of cyclic strain history or aging effects, rather than more complex metallurgical phenomena, the Rockwell "A" hardness was determined for several conditions using halves of broken Charpy specimens. An examination of these results shown in Figure 13 revealed a slight but significant trend toward greater hardness with increasing transition temperature.

An evaluation of some of the tensile specimens by electron microscopy is given in Appendix A.

As noted above, some qualifications are to be noted with regard to the Charpy impact test results following *static* deformation at 350°F. Since these specimens were possibly erroneously machined from a second plate of A-212B, and were tested in the as-received condition without stress relief, or a pretest age, there is some question regarding the validity of comparing the two sets of results. Tests to evaluate the influence of the variables of stress relief at 1050°F for 1-1/2 hours, or a pretest at 350°F for 24 hours indicates that these variables could increase the 50% FATT by perhaps 10°F; this is within the data scatter band of the Charpy impact test, and presumably has little influence. The possibility that this plate represents a second plate of unknown virgin properties is relevant, and this possibility is strengthened by the rather high but not unusual maximum energy values for the static tests.

Comparison of the notch bend properties of this study with those obtained by Burdekin[4] suggest generally similar results for the influence of temperature on notch strength; however, in that case, low stress fracture with subsequent arrest was noted in several instances. Of most significance in these prior tests was the apparent and strong effect of aging on the crack-opening-displacement (COD), or notch strain prior to fracture. As noted previously, the transition from low-to-high COD increased about 195°F for the cold-bent and aged specimens relative to those stress-relieved to remove these effects. Since the notch opening in these tests was not measured it is not possible to compare Burdekin's and these results directly. However, Burdekin's work, particularly the incidence of low stress crack arrest suggests that the few tests made in this study may not be conclusively and generally definitive.

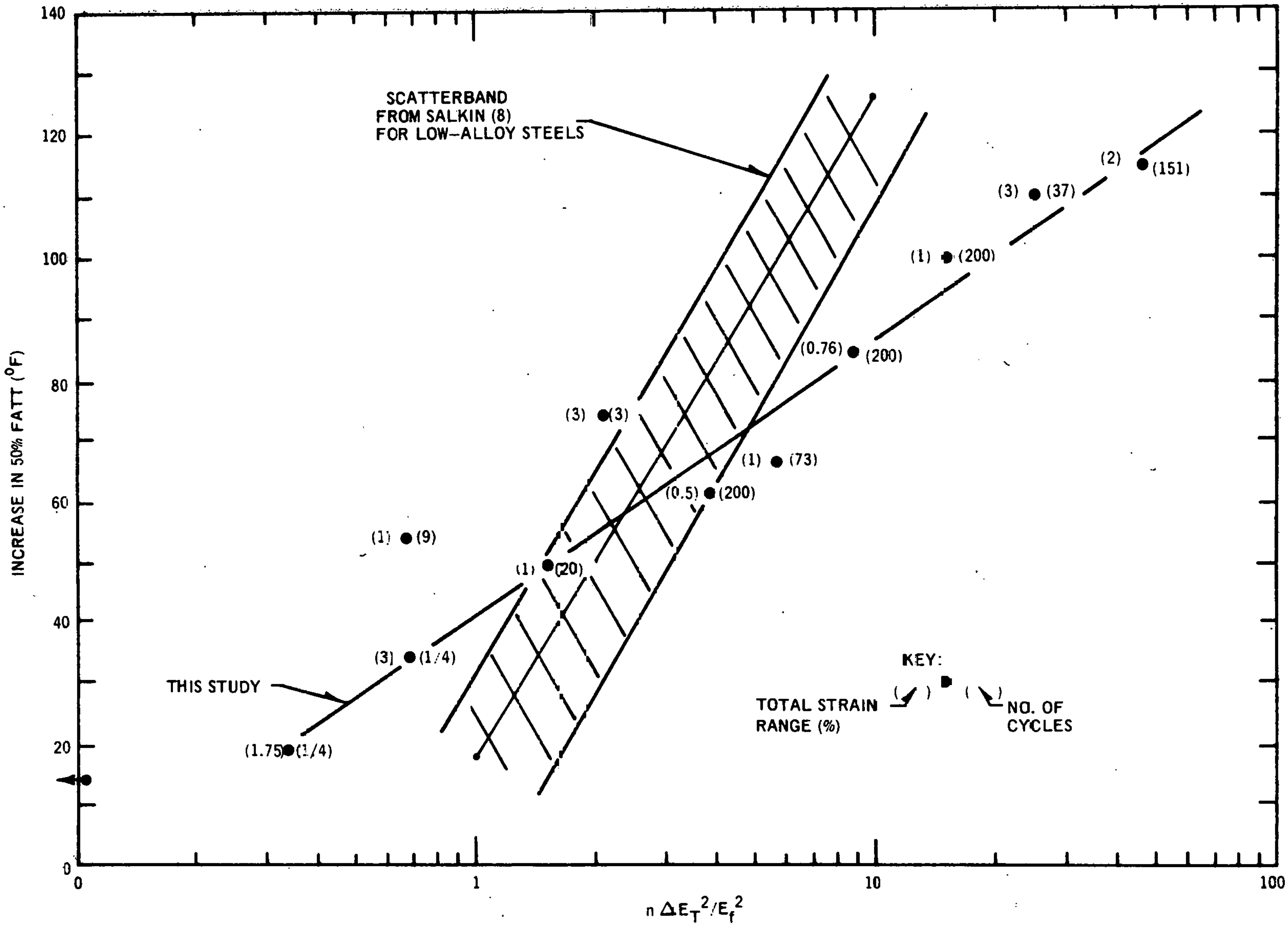

Figure 12 Correlation of Increase in 50% FATT with Cyclic Strain History Parameter

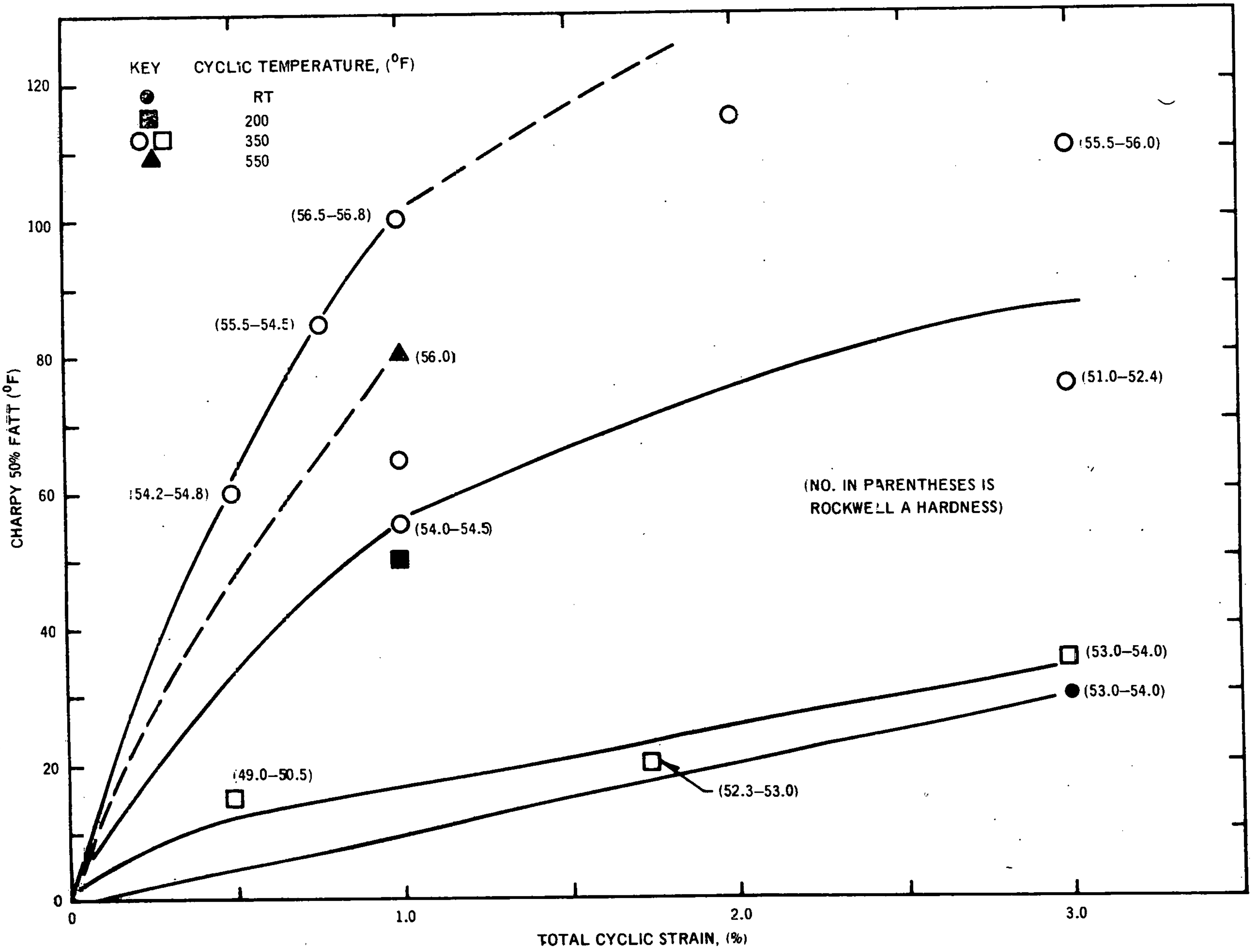

Figure 13. Correlation of Charpy 50% FATT with Total Cyclic Strain Range Illustrating Hardness Changes - See Figure 8

7. SUMMARY AND CONCLUSIONS

The influence of both static and cyclic strain aging on the Charpy impact properties of a 0.24% carbon steel (A-212B) was determined. It was observed that both static strain aging in tensile specimens as reflected in a minimum in ductility or a maximum in strength occurs in the temperature range 300 to 400°F for this steel. Also, it appears that this temperature corresponds to that at which a maximum is observed in the Charpy 50% FATT following a given cyclic strain aging condition.

Examination of the influence of strain range and number of cycles indicates both to be important variables. A maximum shift of about 115°F in 50% FATT was observed after 151 cycles at ±1.0% strain at 350°F. At 550°F, less change occurs in the shift of the Charpy transition temperature, i.e., ±0.5% for 200 cycles led to a shift of 80°F whereas for equivalent straining at 350°F the change in 50% FATT was 100°F.

Examination of the influence of a locally cyclically strain-aged embrittled region in a mildly notched bend bar indicates no apparent influence on notch bend strength at fracture for the range of conditions tested. This phenomenon which is contrary to that observed previously by others may result from a lesser extent of embrittlement in these specimens, and should not be considered as a general effect.

REFERENCES

1. Lankford, W. T., "Effect of Cold Work on the Mechanical Properties of Pressure Vessel Steels," *Welding Journal Research Supplement,* April 1956, p. 195s ff.
2. Terazawa, K., and Otari, M., "Effect of High Temperature Prestraining on Notch Toughness of Steel," *Int. Institute of Welding,* Doc. No. IX-286-61, 1961.
3. Mylonas, C., and Rackey, K. C., "Exhaustion of Ductility by Hot Straining—An Explanation of Fracture Initiation Close to Welds," *Welding Jnl. Res. Suppl.,* **40,** July 1961, p. 306s.
4. Burdekin, F. M., "The Initiation of Brittle Fracture in Structural Steels," *Welding Engineer,* October 1967.
5. Kiefner, J. F., and Munse, W. H., "Influence of Thermal and Strain Cycling on Fracture Susceptibility of Mild Steel," *U. of Illinois Report,* February 1967.
6. Forrest, P. G., "Effect of Fatigue Stressing on the Susceptibility of Steel to Brittle Fracture," *The Engineer,* July 1963.
7. Susukida, H., and Ando, T., "Effect of Low Cycle Fatigue on the Brittle Fracture of Steel," *The Ninth Japan Congress on Testing Materials,* March 1966.
8. Salkin, R. V., *The Effect of Low Cycle Fatigue and Neutron Irradiation on the Mechanical Properties of Low Alloyed Steels,* Presented at 13th Annual Meeting of American Nuclear Society, San Diego, California, June 11, 1967.
9. Powers, A. E., *The Effect of Plastic Strain Cycling on the Mechanical Properties of Type A302B Steel,* General Electric Company, KAPL Materials Engineering Memorandum No. 234, June 1969.
10. Coffin, L. F. Jr., "The Effect of Quench-Aging and Cyclic Strain-Aging on Low Carbon Steel," *Jnl. of Basic Eng., Trans. ASME,* **87,** June 1965, p. 351.

ACKNOWLEDGMENT

The advice and counsel of Dr. L. F. Coffin in the problem recognition and in the experimental design of the cyclic strain aging program is gratefully acknowledged.

APPENDIX A
ELECTRON MICROSCOPY OF STRAIN-AGED PLAIN CARBON STEEL

To supplement the study of the effect of static and cyclic strain aging on the Charpy impact properties of a carbon steel, several of the specimens were examined by electron microscopy. The objective of this aspect of the work was to determine whether the extent of strain aging and the associated increase in transition temperature could be correlated with concomitant structural changes. Although it is believed that maximum effects are related to rather subtle structural modifications, precipitates have been reported in some cases following prolonged strain aging. It has also been demonstrated that dislocation density is dependent on the extent of strain aging occurring during a test.[1] Accordingly, specimens have been examined for evidence of precipitation and changes in dislocation density and dislocation configuration.

A.1 RESULTS

Relief replicas were prepared from tensile specimens deformed to failure at RT, 300°F, and 490°F. Areas close to the fracture and in the undeformed grips were examined. No evidence of precipitation was detected and there were no significant structural changes as a result of the strain and temperature exposure. Figure A-1 shows examples of the structure close to the fracture for the three test temperatures. The micrographs show regions of both ferrite and pearlite.

Examination of thin foils prepared by electrolytic polishing of transverse sections cut from close to the fracture of these same specimens, where the local strains were between 10 and 20%, revealed some dislocation tangling and the beginning of cell formation. Figure A-2 illustrates the type of dislocation structure obtained at the three test temperatures. In general, after deformation at RT, the dislocations tended to be relatively straight. A number of fairly well defined sub-boundaries consisting of dislocation nets were observed [Figure A-2 (A)]. At the higher test temperatures [Figure A-2 (B) and (C)] far more dislocation tangling was apparent and small areas of fairly dense dislocation structures indicated an early stage of cell formation. No significant difference was observed in the specimens deformed at 300°F and 490°F. These observations are rather similar to previous reports of the effect of deformation temperature on the dislocation structure of α-iron[2-4] where the tendency to form cells increased with increasing strain and increasing temperature up to about 500°F.

The maximum increase in transition temperature for this material was obtained after cycling at 350°F. Thin foils were therefore prepared from parallel to the initial rolling plane for several specimens cycled at this temperature. In addition, one foil was examined for each of the other test temperatures. The cycling conditions and the measured increases in 50% FATT for these specimens are described below:

Temperature (°F)	Strain Range (%)	Cycles	Δ FATT (°F)
Room	0.5	20	30
350	1.5	37	110
350	0.5	200	100
350	0.38	200	85
490	0.5	200	80

Figure A-3 shows the dislocation structure and illustrates rather well defined cells approximately 0.5 μm diameter in all cases for the three specimens cycled at 350°F. No significant structural differences were observed for the different cyclic exposures. The structure in the specimen cycled at RT is shown in Figure A-4. In general, the cells appeared to be at an earlier stage of formation with considerable tangling within them. After cycling at 490°F, the dislocations have formed a very distinctive elongated cellular structure shown in Figure A-5. The dark contrast at the cell walls indicates a very high dislocation density and the straight dislocation segments within the cells demonstrate continued accumulation of plastic strain.

A.2 DISCUSSION

The extent and morphology of dislocation cell formation appears to depend on the temperature and deformation mode. However, with the limited number of observations made, it is not possible to relate the structure directly to the measured increase in transition temperature. Although the specimens tested at 350°F have similar transition temperatures and similar cellular development, the specimen tested at 490°F would clearly not fit into a general pattern relating structure and FATT. It is possible that the type of dislocation configuration is mainly controlled by the crystal structure and the deformation conditions, rather than resulting from dislocation-interstitial reaction.

For example, decarburizing has been shown not to significantly affect the dislocation structure of α-iron deformed at various temperatures in tension.[3] It seems probable, therefore, that the measured FATT cannot be related uniquely to the dislocation structure. Among other factors, the density of mobile dislocations, which cannot be determined from an electron micrograph and will depend on the extent of dislocation locking, must be important in determining the response to any subsequent mechanical property test.

REFERENCES

1. Baird, J. D., and Mackenzie, C. R., *J.I.S.I.,* **202,** (1964), 427.
2. Carrington, W., Hale, K. F., and McLean, D., *Proc. Roy. Soc.,* **259,** (1960), 203.
3. Brandon, D. G., and Nutting, J., *J.I.S.I.,* **190,** (1960), 160.
4. Keh, A. S., and Weissman, S., "Electron Microscopy and Strength of Crystals," *Interscience,* New York, (1963), 231.

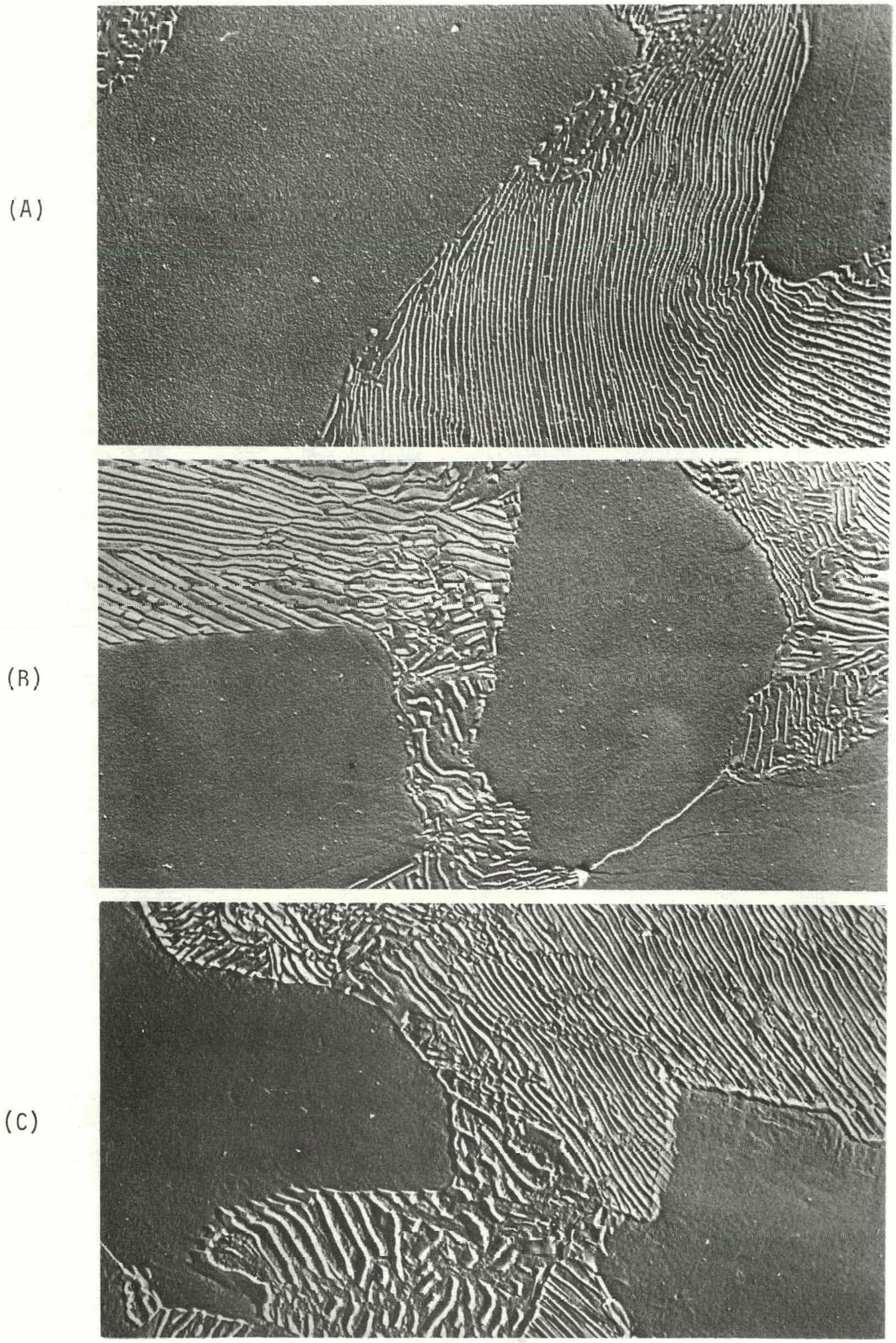

Figure A-1. Relief Replicas Taken From Close to Fracture of Specimens Deformed in Tension at A) RT B) 300° F and C) 490° F

X5000

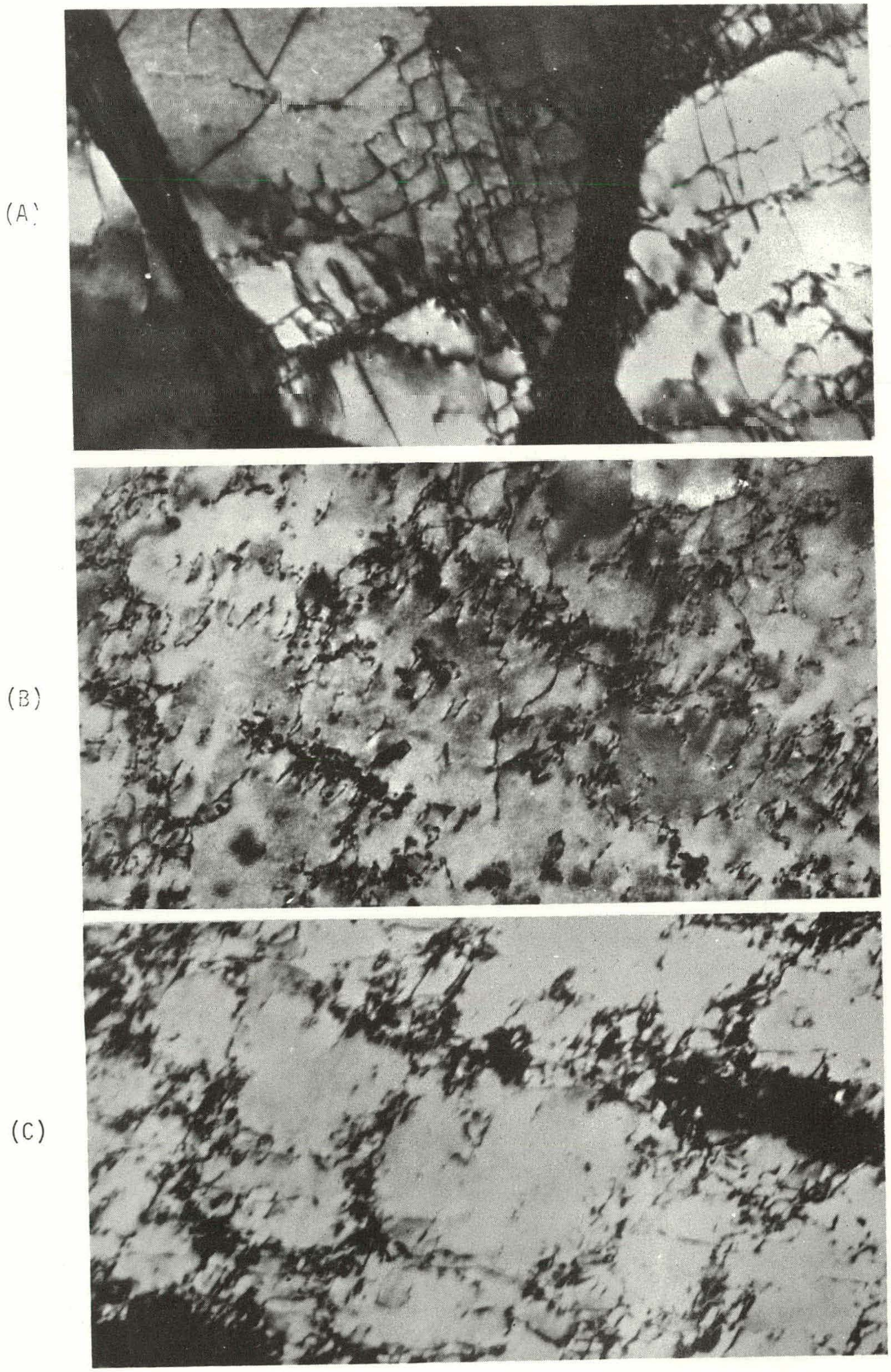

Figure A-2. Effect of Temperature on Dislocation Arrangement After Tensile Deformation. A) RT ~ 20% B) 300°F ~ 10% C) 490°F ~ 15%

X75000

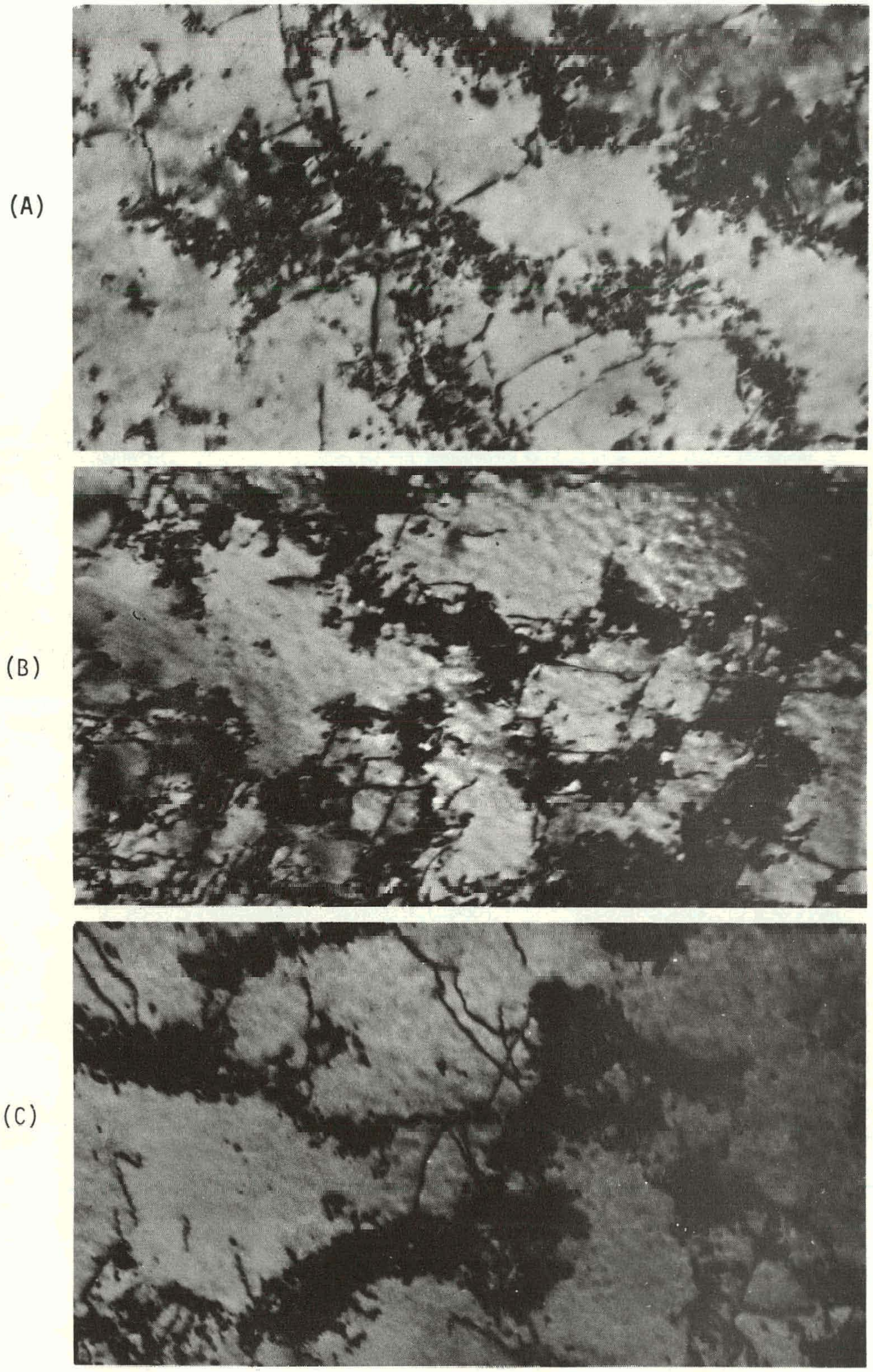

Figure A-3. *Cell Formation Following Fatigue at 350° F A) 37 Cycles at 1.5% B) 200 Cycles at 0.5% C) 200 Cycles at 0.38%.* *X75000*

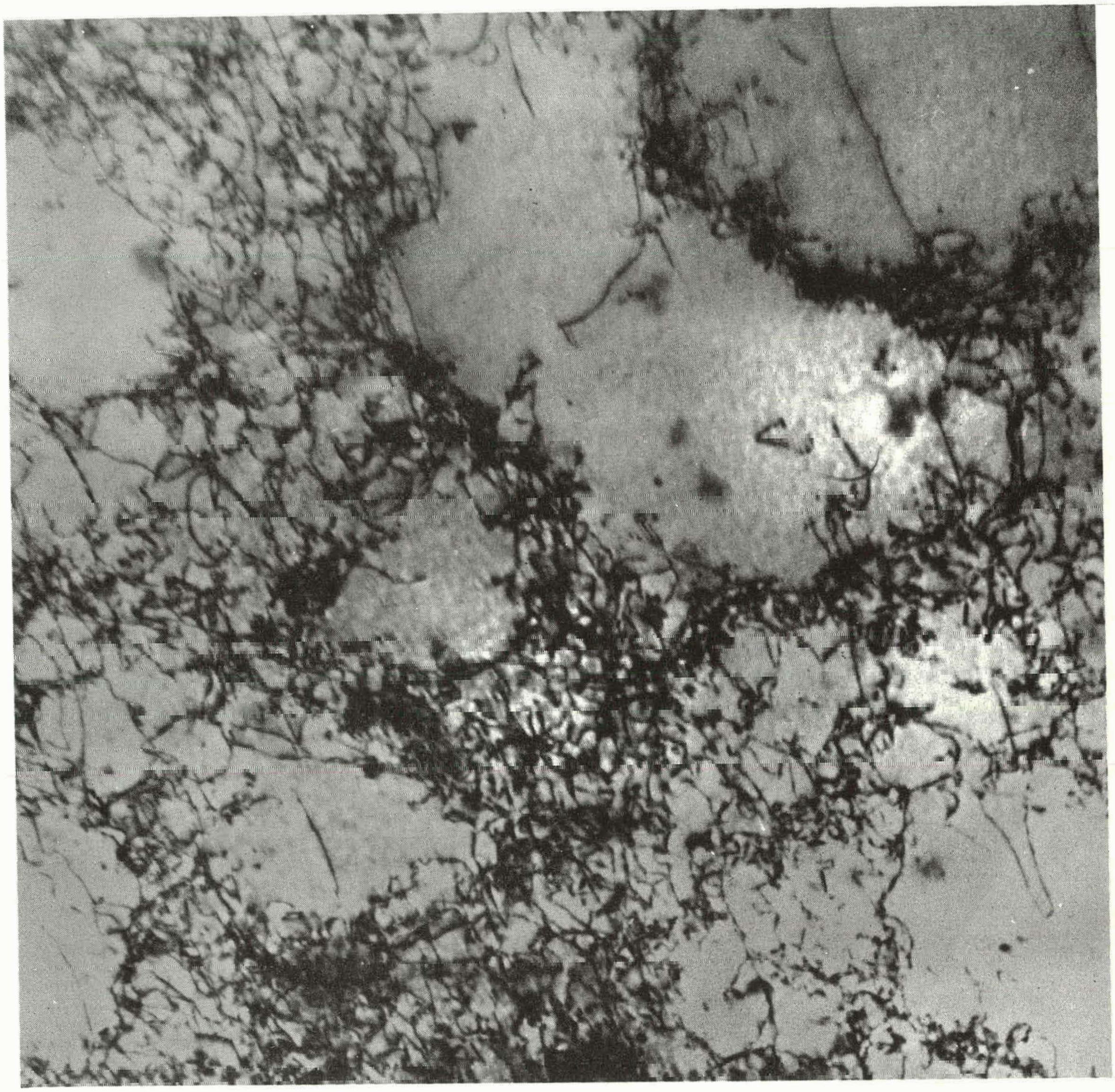

Figure A-4. Cell Formation Following Fatigue at RT for 20 Cycles at 0.5%

X75000

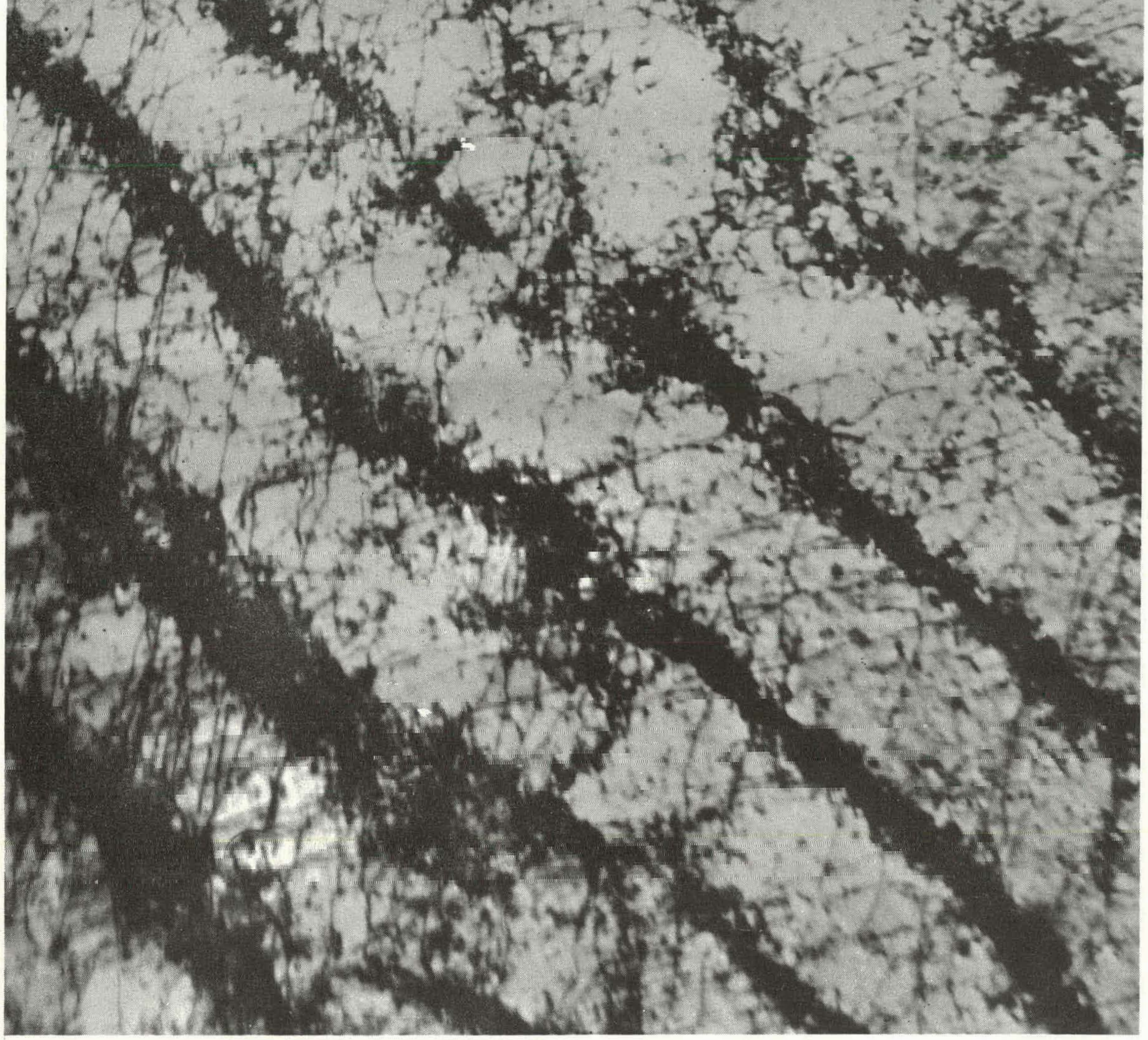

Figure A-5. Elongated Cells Formed After Fatigue at 490° F for 200 Cycles at 0.5%

The series of dark bands going diagonally across this micrograph are cell walls containing a high density of dislocations. Within the cells, a much lower density of relatively straight dislocation segments is present.

X75000

DISTRIBUTION

Aerojet General 1
Engineering Division
Sacramento Plant
Sacramento, California 95801
Attn. Dr. F.J. Climent

Advisory Committee on Reactor Safeguards 1
Dr. Spencer H. Bush
Consultant to the Director
Battelle Memorial Institute
Pacific Northwest Laboratory
Richland, Washington 99352

Advisory Committee on Reactor Safeguards 1
Mr. Harold Etherington
84 Lighthouse Drive
Jupiter, Florida 33458

Advisory Committee on Reactor Safeguards 1
Dr. William L. Faith
2540 Huntington Drive
San Marino, California 91108

Advisory Committee on Reactor Safeguards 1
Dr. Chester P. Siess
Department of Civil Engineering
3129 Civil Engineering Bldg.
University of Illinois
Urbana, Illinois 61801

Advisory Committee on Reactor Safeguards 1
Dr. Stephen H. Hanauer
Professor of Nuclear Engineering
606 Dougherty Hall
University of Tennessee
Knoxville, Tennessee 37916

Advisory Committee on Reactor Safeguards 1
Dr. Joseph M. Hendrie
Nuclear Engineering Department
Brookhaven National Laboratory
Upton, New York 11973

Advisory Committee on Reactor Safeguards 1
Dr. Herbert S. Isbin
Department of Chemical Engineering
University of Minnesota
Minneapolis, Minnesota 55455

Advisory Committee on Reactor Safeguards 1
Mr. Harold G. Mangelsdorf
78 Knollwood Road
Short Hills, New Jersey 07078

Advisory Committee on Reactor Safeguards 1
Dr. Harry O. Monson, Senior Engineer
Laboratory Director's Office
Argonne National Laboratory
9700 South Cass Avenue
Argonne, Illinois 60439

Advisory Committee on Reactor Safeguards 1
Dr. Arlie A. O'Kelly
2421 West Rowland Avenue
Littleton, Colorado 80120

Advisory Committee on Reactor Safeguards 1
Dr. David Okrent, Senior Physicist
Laboratory Director's Office
Argonne National Laboratory
9700 South Cass Avenue
Argonne, Illinois 60439

Advisory Committee on Reactor Safeguards 1
Dean Nunzio J. Palladino
College of Engineering
The Pennsylvania State University
101 Hammond Building
University Park, Pennsylvania 16802

Advisory Committee on Reactor Safeguards 1
Dr. William R. Stratton
Los Alamos Scientific Laboratory
P. O. Box 1663
Los Alamos, New Mexico 87544

Advisory Committee on Reactor Safeguards 1
Dr. Carroll W. Zabel
Director of Research
University of Houston
Cullen Boulevard
Houston, Texas 77004

Mr. Raymond F. Fraley 3
Executive Secretary
Advisory Committee on Reactor Safeguards
U.S. Atomic Energy Commission
Room 1034-H
Washington, D.C. 20545

Argonne National Laboratory 1
9700 South Cass Avenue
Argonne, Illinois
Attn: Mr. Paul G. Shewmon

Argonne National Laboratory 1
9700 South Cass Avenue
Argonne, Illinois
Attn: Dr. P. Lottes

Argonne National Laboratory 1
9700 South Cass Avenue
Argonne, Illinois
Attn: Dr. C.E. Dickerman

Argonne National Laboratory 1
9700 South Cass Avenue
Argonne, Illinois
Attn: Dr. R.O. Ivins

Argonne National Laboratory 1
9700 South Cass Avenue
Argonne, Illinois
Attn: Dr. S. Fistedis

Argonne National Laboratory 1
9700 South Cass Avenue
Argonne, Illinois
Attn: Dr. R.C. Vogel

Argonne National Laboratory 1
9700 South Cass Avenue
Argonne, Illinois
Attn: LMFBR Program Office

Argonne National Laboratory 2
9700 South Cass Avenue
Argonne, Illinois
Attn: Mr. A. Amorosi

Argonne National Laboratory 1
9700 South Cass Avenue
Argonne, Illinois
Attn: Dr. L. Baker

Atomic Energy Commission 1
Division of Reactor Development and Technology
Washington, D.C. 20545
Attn: Col. R.L. Ednie
Asst. Director for Army Reactors

Atomic Energy Commission 1
Division of Reactor Development and Technology
Washington, D.C. 20545
Attn: Mr. M.A. Rosen
Asst. Director for Plant Engineering

Atomic Energy Commission 1
Division of Reactor Development and Technology
Washington, D.C. 20545
Attn: Mr. M.J. Whitman
Asst. Director for Program Analysis

Atomic Energy Commission 1
Division of Reactor Development and Technology
Washington, D.C. 20545
Attn: Dr. E.E. Sinclair
Asst. Director for Reactor Technology

Atomic Energy Commission 1
Division of Reactor Development and Technology
Washington, D.C. 20545
Attn: Mr. A. Giambusso
Asst. Director for Project Management

Atomic Energy Commission 1
Division of Reactor Development and Technology
Washington, D.C. 20545
Attn: Mr. E.E. Kintner
Asst. Director for Reactor Engineering

Atomic Energy Commission 1
Division of Reactor Development and Technology
Washington, D.C. 20545
Attn: Mr. J. W. Crawford
Asst. Director for Engineering Standards

Atomic Energy Commission 1
Division of Compliance, Region IV
10395 West Colfax Avenue
Denver, Colorado 80215
Attn: Mr. John W. Flora

Atomic Energy Commission 1
Division of Compliance
Washington, D.C. 20545
Attn: Mr. L. Kornblith, Jr.

Atomic Energy Commission 1
Division of Operational Safety
Washington, D.C. 20545
Attn: Mr. H. Gilbert

Atomic Energy Commission 10
Division of Reactor Standards
Washington, D.C. 20545
Attn: Mr. E.G. Case

Atomic Energy Commission 1
Division of Reactor Standards
Washington, D.C. 20545
Attn: Mr. M. Bolotsky

Atomic Energy Commission 1
Division of Reactor Standards
Washington, D.C. 20545
Attn: Mr. A.B. Holt

Atomic Energy Commission 1
Division of Reactor Standards
Washington, D.C. 20545
Attn: Mr. R. Waterfield

Atomic Energy Commission 1
Division of Reactor Standards
Washington, D.C. 20545
Attn: Dr. G. Burley

Atomic Energy Commission 1
Division of Reactor Standards
Washington, D.C. 20545
Attn: Mr. R. Impara

Atomic Energy Commission 1
Water Projects Branch
Division of Reactor Development and Technology
Washington, D.C. 20545
Attn: Mr. W.H. Layman

Atomic Energy Commission 2
Naval Reactors Branch
Division of Reactor Development and Technology
Washington, D.C. 20545
Attn: Mr. R.S. Brodsky

Atomic Energy Commission 7
Division of Reactor Development and Technology
Washington, D.C. 20545
Attn: A.J. Pressesky

Atomic Energy Commission 5
Division of Reactor Development and Technology
Washington, D.C. 20545
Attn: Mr. S.A. Szawlewicz

Atomic Energy Commission 1
Division of Reactor Development and Technology
Washington, D.C. 20545
Attn: Mr. R.R. Newton

Atomic Energy Commission 1
Division of Production
Washington, D.C. 20545
Attn: Mr. George B. Pleat

Atomic Energy Commission 1
c/o Gulf General Atomic, Inc.
P.O. Box 608
San Diego, California 92112
Attn: Mr. Russell H. Ball

Atomics International 2
P.O. Box 309
Canoga Park, California
Attn: Dr. H. Morewitz

Babcock & Wilcox Company 1
Washington Operations Office
1725 I Street, N.W.
Washington,D.C. 20006

Babcock & Wilcox Company 1
P.O. Box 1260
Lynchburg, Virginia
Attn: Mr. Robert Wascher

Battelle Memorial Institute 2
505 King Avenue
Columbus, Ohio 43201
Attn: Dr. D.N. Sunderman

Battelle Memorial Institute 1
505 King Avenue
Columbus, Ohio 43201
Attn: Dr. D.L. Morrison

Battelle Memorial Institute 2
505 King Avenue
Columbus, Ohio 43201
Attn: Mr. S. Paprocki

Battelle Memorial Institute 1
505 King Avenue
Columbus, Ohio 43201
Attn: Mr. A.R. Duffy

Brookhaven National Laboratory 1
Upton, Long Island, New York 11973
Attn: A.W. Castleman

University of California 1
Institute of Engineering Research
Berkeley, California 94704
Attn: Prof. V.E. Schrock

University of California 1
Institute of Engineering Research
Berkeley, California 94704
Attn: Prof. H.A. Johnson

Canoga Park Area Office 1
P.O. Box 591
Canoga Park, California 91305
Attn: Mr. R.L. Morgan RDT Senior Site Rep.

Combustion Engineering, Inc. 1
Nuclear Division
P.O. Box 500
Windsor, Connecticut 06095
Attn: Mr. M.F. Valerino

Chicago Operations Office 1
Atomic Energy Commission
9800 South Cass Avenue
Argonne, Illinois 60439
Attn: Mr. D.M. Gardiner

Douglas United Nuclear 1
Richland, Washington
Attn: Mr. John Riches

Harvard Air Cleaning Laboratory 1
Harvard University
665 Huntington Avenue
Boston, Massachusetts 02190

IIT Research Institute 1
10 W. 35th Street
Chicago, Illinois 60616
Attn: Dr. T.A. Zaker

IIT Research Institute 1
10 W. 35th Street
Chicago, Illinois 60616
Attn: Mr. E.V. Gallagher

Idaho Operations Office 2
Atomic Energy Commission
P.O. Box 2108
Idaho Falls, Idaho 83401
Attn: Mr. D. Williams

Liquid Metal Engineering Center 1
c/o Atomics International
P.O. Box 309
Canoga Park, California 91304
Attn: R.W. Dickinson

Los Alamos Scientific Laboratory 1
P.O. Box 1663
Los Alamos, New Mexico 87544
Attn: Mr. J.H. Russel, K Division

MPR Associates, Inc. 1
1140 Connecticut Avenue, N.W.
Washington, D.C. 20036
Attn: Mr. T. Rockwell III
Chairman AIF Safety Task Force

National Bureau of Standards 1
Washington, D.C. 20545
Attn: Dr. C. Muehlhause

Naval Ordnance Laboratory 1
White Oak
Silver Spring, Maryland
Attn: Mr. James Proctor

North Carolina State University 1
Department of Mechanical Engineering
Raleigh, North Carolina 27607
Attn: Prof. M.N. Ozisik

Nuclear Fuels Services 1
West Valley, New York 14171

Oak Ridge Operations Office 1
Atomic Energy Commission
Oak Ridge, Tennessee 37830
Attn: Mr. W.L. Smalley

Oak Ridge National Laboratory 1
Nuclear Safety Information Center
P.O. Box Y
Oak Ridge, Tennessee 37830
Attn: Mr. Joel Buchanan

Chemical Technology Division 1
Oak Ridge National Laboratory
P.O. Box Y
Oak Ridge, Tennessee 37830
Attn: Mr. D. Ferguson

Chemical Technology Division 1
Oak Ridge National Laboratory
P.O. Box Y
Oak Ridge, Tennessee 37830
Attn: Mr. R. Blanco

Oak Ridge National Laboratory 2
P.O. Box Y
Oak Ridge, Tennessee
Attn: HTGR Safety Program Office

Oak Ridge National Laboratory 4
P.O. Box Y
Oak Ridge, Tennessee
Attn: Mr. W. B. Cottrell

Oak Ridge National Laboratory 1
P.O. Box Y
Oak Ridge, Tennessee
Attn: Mr. P. Rittenhouse

Pacific Northwest Laboratories 1
P.O. Box 099
Richland, Washington 99352
Attn: Mr. G. Rogers

Pacific Northwest Laboratories 1
P.O. Box 999
Richland, Washington 99352
Attn: Mr. J.C. Spanner

Pacific Northwest Laboratories 1
P.O. Box 999
Richland, Washington 99352
Attn: Dr. J. Batch

Pacific Northwest Laboratories 2
P.O. Box 999
Richland, Washington 99352
Attn: Mr. R. Nightingale

Pacific Northwest Laboratories 1
P.O. Box 999
Richland, Washington 99352
Attn: Mr. L. Schwendiman

Pacific Northwest Laboratories 1
P.O. Box 999
Richland, Washington 99352
Attn: Mr. E.R. Astley, Mgr. FFTF

Idaho Nuclear Corporation 1
P.O. Box 1845
Idaho Falls, Idaho 83401
Attn: Mr. Curt Haire

Idaho Nuclear Corporation 2
P. O. Box 1845
Idaho Falls, Idaho 83401
Attn: Mr. S. O. Johnson

Idaho Nuclear Corporation 2
P.O. Box 1845
Idaho Falls, Idaho 83401
Attn: Mr. H. L. Coplen

Idaho Nuclear Corporation 1
P. O. Box 1845
Idaho Falls, Idaho 83401
Attn: Mr. O. F. Brockett

Idaho Nuclear Corporation 3
P. O. Box 1845
Idaho Falls, Idaho 83401
Attn: Water Reactor Safety Program
Office, Mr. G. O. Bright, Mgr.

Richland Operations Office 1
P.O. Box 500
Richland, Washington 99352
Attn: Mr. C. Robinson

Richland Operations Office 1
P.O. Box 500
Richland, Washington 99352
Attn: Mr. A.S. Waterhouse

Richland Operations Office 1
P.O. Box 500
Richland, Washington 99352
Attn: Mr. A. Brunstad

San Francisco Operations Office 1
Atomic Energy Commission
2111 Bancroft Way
Berkeley, California 94704
Attn: Mr. C.V. Backlund

Savannah River Laboratories 1
E.I. duPont deNemours and Company
Aiken, South Carolina 29802
Attn: Mr. A.H. Peters

TRW Inc. 1
TRW Systems Group
One Space Park
Redondo Beach, California 90278
Attn: Dr. D. B. Langmuir

TRW Inc. 1
TRW Systems Group
One Space Park
Redondo Beach, California 90278
Attn: Mr. S.M. Zivi

Westinghouse Electric Corporation 1
Atomic Power Division
P.O. Box 355
Pittsburgh, Pennsylvania 15230
Attn: Mr. R.A. Wiesemann

Westinghouse Electric Corporation 1
Atomic Power Division
P.O. Box 355
Pittsburgh, Pennsylvania 15230
Attn: Dr. D. Fletcher

Westinghouse Electric Corporation 1
Atomic Power Division
P.O. Box 355
Pittsburgh, Pennsylvania 15230
Attn: Dr. E. Beckjord

Westinghouse Electric Corporation 1
P.O. Box 19218
Tampa, Florida 33616
Attn: Mr. A. Lohmeier

Southern Nuclear Engineering, Inc. 1
P.O. Box 10
Dunedin, Florida 33528
Attn: Mr. Gilbert Brown

Holmes & Narver, Inc. 1
828 South Figueroa St.
Los Angeles, California 90017
Attn: B. Shimizu

Mr. Edward T. Wessel 1
Research and Development Center
Westinghouse Electric Corporation
Beulah Road, Churchill Boro
Pittsburgh, Pennsylvania 15235

Dr. William E. Cooper 1
Teledyne Materials Research
303 Bear Hill Road
Waltham, Massachusetts

Roger W. Staehle 1
Metallurgy Department
Ohio State University
Columbus, Ohio

Mr. Ralph Jones 1
Division of Reactor Development
U.S. Atomic Energy Commission
Washington 25, D.C.

Mr. H.K. Marks 1
Room 2N83
Department of the Navy
Washington, D.C.

H. Thielsch 1
140 Shaw Avenue
Cranston 5, Rhode Island

Mr. F.M. Moschine 1
Westinghouse Electric Company
Atomic Power Department
P.O. Box 355
Pittsburgh, Pennsylvania 15230

Dr. P. L. Pfenningwerth 1
Bettis Atomic Power Laboratory
P.O. Box 79
West Mifflin, Pennsylvania 15122

Professor C.E. Taylor 1
Department of Theoretical and Applied Mechanics
University of Illinois
Urbana, Illinois

Mr. E. Beauchamp-Nobbs 1
U.S. Marine Engineering Laboratory
Annapolis, Maryland

U.S. Atomic Energy Commission 3
Division of Technical Information Extension
P.O. Box 62
Oak Ridge, Tennessee

U.S. Atomic Energy Commission 1
Division of Reactor Licensing
Washington, D.C. 20545
Attn: S.S. Pawlicki

USAEC Site Representative 1
General Electric Company
Sunnyvale, California 94086
Attn: Joel Levy, Senior Site Rep.

Mr. B.L. Greenstreet 1
P.O. Box Y
Oak Ridge National Laboratory
Oak Ridge, Tennessee

Mr. F.J. Witt 1
P.O. Box Y
ORNL - Oak Ridge, Tennessee

Commonwealth Edison Company 2
Dresden Nuclear Power Station
Rural Route 1
Morris, Illinois 60450
Attn: H.K. Hoyt

Commonwealth Edison Company 3
System Mechanical and Structural Engineer
72 West Adams Street
Chicago, Illinois 60690
Attn: N.A. Kershaw

United Kingdom Atomic Energy Authority 1
Reactor Materials Laboratory
Wigshaw Lane, Culcheth
Warrington, Lancs.
England
Attn: R.W. Nichols

Atomic Energy of Canada Limited 1
Chalk River Nuclear Laboratories
Chalk River, Ontario, Canada
Dr. George Pon

Mr. Robert D. Wylie 1
Department of Materials Engineering
Southwest Research Institute
8599 Culebra Road
San Antonio, Texas 78228

O.A. Kellerman 1
Institut Fur Reaktorsicherheit
Der Technischen Uberwachungs
Vereine, e.V.
5 Koln - Ehrenfeld, Lukasstr. 90
West Germany

C. A. G. Phillips 1
U.K.A.E.A. Safeguards Division
Authority Health & Safety Branch
Risley, Warrington, Lancashire
England

Knolls Atomic Power Laboratory 1
P. O. Box 1072
Schenectady, New York 12301
Attn: Dr. Robert A. Barnes

Reactor Materials Branch 1
Metallurgy Division
Naval Research Laboratory
Washington, D. C. 20545
Attn: Mr. L. E. Steele

Department of Material Science & Engineering 1
Hearst Mining Building
University of California
Berkeley, California
Attn: Mr. William W. Gerberich

United Engineers and Constructors, Inc. 1
1401 Arch Street
Philadelphia, Pennsylvania 19105
Attn: Mr. John Crowley

Argonne National Laboratory 1
9700 South Cass Avenue
Argonne, Illinois
Attn: Mr. Craig Cheng

AEG Telefunken 1
AEC Hochhaus Sued
6 Frankfurt/Main 70
West Germany
Attn: Mr. Dieter Ewers

Division of Reactor Development & Technology 1
U.S. Atomic Energy Commission
Washington, D.C. 20545
Attn: J. R. Hunter